N71-38746
NASA CR 120781
AMS 987

Theoretical Investigation on Transverse Mode Combustion Instability for Liquid Propellant Rockets

by

Jean H. Lorenzetto and Luigi Crocco

PRINCETON UNIVERSITY

prepared for

NATIONAL AERONAUTICS AND SPACE ADMINISTRATION

NASA Lewis Research Center
Grant NGL 31-001-155
Marcus Heidmann, Project Manager
Chemical Rockets Division

1. Report No. NASA CR 120781	2. Government Accession No.	3. Recipient's Catalog No.
4. Title and Subtitle THEORETICAL INVESTIGATION ON TRANSVERSE MODE COMBUSTION INSTABILITY FOR LIQUID PROPELLANT ROCKETS		5. Report Date Sept. 1971
		6. Performing Organization Code
7. Author(s) Jean H. Lorenzetto and Luigi Crocco		8. Performing Organization Report No.
		10. Work Unit No.
9. Performing Organization Name and Address Princeton University Princeton, New Jersey 08540		11. Contract or Grant No. NGL 31-001-155
		13. Type of Report and Period Covered Contractor Report
12. Sponsoring Agency Name and Address National Aeronautics and Space Administration Washington, D.C. 20546		14. Sponsoring Agency Code
15. Supplementary Notes Project Manager, Marcus F. Heidmann, Chemical Rockets Division, NASA Lewis Research Center, Cleveland, Ohio		

16. Abstract

A mathematical approach is described which provides an analytical solution to the problem of nonlinear transverse combustion instability in a thin annular liquid propellant rocket chamber. Finite chamber lengths are considered as well as a time dependency on the droplet lifetime. Boundary conditions existing at the injector and nozzle eliminate the restrictions of holding mass, energy, and momentum constant with time. A numerical integration of the waveshape equation and employing the Priem-Heidmann droplet evaporation model results in a shock-type periodic solution. Threshold limits corresponding to triggering instability as well as limiting-cycle behavior are found using this approach.

To design for rocket operation as far as possible from the triggering limit this analysis indicates that (1) the combustion should either be spread over the entire length of the combustor or completed in less than 20% of chamber length for the example cited, (2) the chamber length should be as small as possible compared to the mean annulus circumference and (3) the ratio of nozzle entrance to injected velocity should be maximized by injecting the propellant at the lowest velocity and increasing the chamber Mach number.

17. Key Words (Suggested by Author(s))	18. Distribution Statement
Combustion Instability Liquid Rockets	Unclassified - unlimited

19. Security Classif. (of this report)	20. Security Classif. (of this page)	21. No. of Pages	22. Price*
Unclassified	Unclassified	63	$3.00

* For sale by the National Technical Information Service, Springfield, Virginia 22151

NASA-C-168 (Rev. 6-71)

FOREWORD

The research described in this report was supported by NASA Grant NGL 31-001-155 and monitored by Mr. Marcus Heidmann. Early theoretical efforts were performed by Professor Crocco both at Princeton University and while on leave. The work was completed by Mr. Jean Lorenzetto under Professor Crocco's direction. Assistance in the preparation of this report was provided by Mr. David T. Harrje, Senior Research Engineer and Lecturer at Princeton University.

SUMMARY

A quantitative understanding of the combustion process associated with transverse mode combustion instability in an annular liquid rocket motor is the objective of this theoretical research. Emphasis is on the nonlinear aspects of the phenomena. The gas dynamic equations for the annular motor are developed and represent a considerable simplification when compared to the cylindrical chamber. The equations are solved by the technique of expansion in powers of a small parameter related to the perturbation amplitude. Since the source term is strongly dependent on the comparative magnitude of the transverse perturbation v and the steady-state relative axial velocity $u_{\ell} - \bar{u}$, different ranges of these velocities are considered and conditions for the existence of shock-type periodic solutions is determined.

This theoretical study confirmed that shock-type waves are characteristic of transverse mode instability in an annular chamber as shown experimentally. The design requirements to minimize the occurrence of such instability (apart from requiring solutions such as baffles and acoustic liners) are that: (1) the combustion should either be spread over the entire length of the combustor or completed in less than 20% of chamber length for the example cited, (2) the chamber length should be as small as possible compared to the mean annulus circumference and (3) the ratio of nozzle entrance to injected velocity should be maximized by injecting the propellant at the lowest velocity and increasing the chamber Mach number.

TABLE OF CONTENTS

NOMENCLATURE

A_i	=	injection port area
A	=	function of the parameters: $\bar{u}_n$, ℓ and γ
a	=	sonic velocity
B	=	function of the parameters: $\bar{u}_n$, ℓ and γ
b	=	station in the combustion chamber wherein steady state, $\bar{\nu} = 0$
C	=	constant
C_1	=	constant (see Eq. (18))
C_2	=	constant (see Eq. (18))
c_r	=	reference sonic velocity
D	=	function of the parameters: β, τ, ℓ and γ
f	=	frequency
F	=	general quantity
ΔF	=	jump of the quantity F through the shock
g	=	linear integral function of θ
G	=	integral function of $g(\theta)$
K	=	function of β
ℓ	=	combustion chamber length
M	=	function of θ
$\mathring{m}_i$	=	injection flux per unit area
N^d	=	droplet number density
O( )	=	order of
p	=	pressure
Pr	=	Prandtl number
Q	=	mass source (or evaporation rate)
q	=	gas velocity

q_ℓ = liquid propellant velocity

q_{rel} = relative velocity

r_i = droplet radius at injection

Re = Reynolds number

t = time

u = longitudinal gas velocity

u_ℓ = longitudinal liquid velocity

u_n = gas velocity at nozzle entrance

V = droplet volume (relative to injection droplet volume)

v = circumferential gas velocity

x = longitudinal coordinate

y = circumferential coordinate

$\frac{D}{Dt}$ = substantial derivative

Greek Symbols

α = circumferential coordinate defined as: ft-y

β = ratio of the gas velocity at nozzle entrance to the liquid propellant velocity.

γ = ratio of specific heats

δ = time elapsed from the injection of the droplet

φ = arbitrary function of

ξ = stretching of the longitudinal coordinate

μ = nondimensional injection flux

ν = square root of the relative droplet volume

ρ = gas density

ρ_r = reference gas density

ρ_L = liquid propellant density

$\rho_{\ell i}$ = amount of propellant per unit chamber volume at injection

τ = droplet lifetime

ζ = dummy variable

ϕ = guess function of θ to start the iteration procedure

σ = nondimensional entropy change

θ = stretching of the circumferential coordinate

θ^* = value of θ for which the transversal velocity $v(\theta)$ takes on the mean value v_m

Subscripts

0 = zeroth-order quantity

1 = first-order quantity

2 = second-order quantity

m = corresponding to a mean value along the shock

n = nozzle

α = partial derivative with respect to α

ξ = partial derivative with respect to ξ

θ = partial derivative with respect to θ

x = partial derivative with respect to x

t = partial derivative with respect to t

bar = vector

asterisk = related to the station in the combustion chamber where the steady-state gas velocity is equal to the liquid propellant velocity.

Superscripts

asterisk = dimensional value

bar = steady-state value

prime = perturbation

SECTION I

Introduction

In a liquid propellant rocket motor, the combustion process is never entirely smooth. During the steady-state period between starting and cutoff, fluctuations occur in all important properties (pressure, temperature, velocity, etc.) around the desired operating values. The amplitude of such fluctuations can vary over a wide range, from motor to motor and in one motor for different operating conditions. When the fluctuations are completely random, the operation is classified as "rough" combustion. Combustion instability, on the other hand, consists of organized oscillations, which are maintained and amplified by the combustion process itself.

Theoretical explanations of the causes of combustion instability date back to Rayleigh's analysis. Since that time a number of concepts have been advanced.[1-12] One example is the constant combustion time lag which has proven to be useful in explaining low frequency instability (i.e., interaction between the feed system and combustion chamber). Later Crocco introduced the time varying combustion lag in his analysis of high frequency instability. That approach involved both insensitive and sensitive time lags, the later responding to fluctuations in the chamber conditions. Sirignano analyzed longitudinal mode, nonlinear combustion instability for a combustion time negligible compared to wave travel time in the chamber and for combustion times of the same order of magnitude. Unstable operation was shown possible for both conditions with triggering action initiated whenever a phase existed between energy addition and pressure. Later theoretical studies at Princeton dealt with transverse modes and with concentrated combustion.

A mechanistic approach to the origins of combustion instability was investigated by Priem and Guentert[9] at Lewis Research Center. The approach used the Priem-Heidmann[13] droplet evaporation model as the basic for energy generation. The assumptions used in that mechanistic approach may be briefly stated as:

1) the burning rate was equal to the vaporization rate,

2) the combustion chamber was composed of toroids of a very small thickness, Δr, and length, Δz,

3) and the total mass, momentum and energy in the toroids were constant.

In the present work, which is the subject of this report, the theoretical model of the combustion chamber is an annular geometry and use has been made of the same droplet evaporation model. However, the differences are in the assumptions in that:

1) instead of a one-dimensional toroidal section with a very small thickness and length, here we consider a two-dimensional combustion with a finite length ℓ,

2) in the present model a time dependency for the droplet has been introduced ($\tau = b/u_\ell$, where b is the station at which the droplet vanishes and u_ℓ is the constant liquid velocity),

3) restrictions as to mass, energy and momentum constant with time are no longer necessary because of the boundary conditions existing in the present model at the injector and nozzle entrance planes.

As liquid rocket designs have changed with time one observes that tangential modes have surpassed longitudinal modes in importance, shock waves and other nonlinear behavior have become increasingly important. The purpose of this report is to focus attention on the combustion behavior of an annular chamber to illustrate how the basic mechanism of droplet evaporation together with the chamber gas dynamics can result in combustion instability. Triggering behavior and limit cycle operation are traced to the effect of the pressure oscillations on the combustion processes where the amount of energy feedback is sufficient to balance the energy absorbed by dissipative or other damping processes.

SECTION II
Annular Motor

The mathematical approach which was developed by Crocco for nonlinear transverse mode instability is described in this section.

2.1 Theoretical Model and Assumptions

A combustion chamber geometry corresponding to a constant thin annular cross section followed by a large number of individual small nozzles (Fig. 1) has been chosen. The dependence on the radial coordinate can be disregarded and the only relevant independent variables are the time t, the axial coordinate x and the circumferential coordinate y. The reference length will be chosen equal to the circumferential development of the annulus; the reference velocity is the sonic velocity in the reference state; and the reference time is the ratio of the reference length to the velocity. All other quantities are normalized accordingly.

The fundamental assumptions are the following:

a) The gaseous material contained in the chamber is in the form of gases of perfect combustion. The volume occupied by liquid or vaporized propellants and intermediate combustion products is negligible.

b) The combustion gases are assumed to be thermally and calorically perfect and homocompositional. Viscous effects and heat conduction are disregarded. The combustion immediately follows the propellant evaporation.

c) The droplets have no drag, so that their velocity u_ℓ is constant in space and time.

d) A combustion model has been retained such that the combustion rate which has been assumed to be equal to the droplet evaporation rate, has a law of proportionality with respect to the square root of the Reynolds number[13].

2.2 The Combustion Chamber Equations

Following Crocco's mathematical derivation, we first write the conservation equations for the combustion chamber:

$$\rho_t + \nabla\cdot(\rho \underline{q}) = Q$$

$$\rho\left[\underline{q}_t + (\underline{q}\cdot\nabla)\underline{q}\right] + \frac{\nabla p}{\gamma} = -Q\,(\underline{q} - \underline{q}_\ell)$$

$$\frac{p_t}{\gamma} + \nabla\cdot(p\underline{q}) + \frac{\gamma-1}{2}\left[(\rho q^2)_t + \nabla\cdot(\rho q^2 \underline{q})\right] = Q$$

The right-hand sides of the three equations represent the mass, momentum and energy sources corresponding to the rate of gasification (or combustion rate) Q of the liquid propellants. The expressions for the first and the third actually coincide only because in the nondimensionalization the energy content of any mass generated is taken as unity.

The conservation equations can be transformed to the variables p, $\underline{q}$ and σ (representing a nondimensional entropy change from the reference conditions) by taking $\rho = p^{1/\gamma} e^{-\sigma}$. After rearranging, the new equations can be written in the convenient form:

$$\frac{1}{\gamma} p_t + \frac{1}{\gamma}\,\underline{q}\cdot\nabla p + p\,\nabla\cdot\underline{q} = Q\left[1 - \frac{\gamma-1}{2}\left(2\,\underline{q}_\ell\cdot\underline{q} - q^2\right)\right]$$

$$\underline{q}_t + (\underline{q}\cdot\nabla)\underline{q} + p^{-1/\gamma} e^{\sigma}\,\frac{\nabla p}{\gamma} = -p^{-1/\gamma} e^{\sigma}\, Q\,(\underline{q} - \underline{q}_\ell)$$

$$\sigma_t + \underline{q}\cdot\nabla\sigma = Q\left[\frac{1}{p} - p^{-1/\gamma} e^{\sigma} - \frac{\gamma-1}{2p}\left(2\,\underline{q}_\ell\cdot\underline{q} - q^2\right)\right]$$

The only relevant independent variables are t, x and y. The reference length will be chosen equal to the circumferential development of the annulus. Hence, all physical quantities must be periodic in y with unitary period. The equations for the annular geometry become:

$$\frac{p_t}{\gamma} + u \frac{p_x}{\gamma} + v \frac{p_y}{\gamma} + p\,(u_x + v_y) = Q\left[1 - \frac{\gamma-1}{2}\left(2u_\ell u - u^2 - v^2\right)\right]$$

$$u_t + u u_x + v u_y + p^{-1/\gamma} e^{\sigma} \frac{p_x}{\gamma} = -p^{-1/\gamma} e^{\sigma} Q\,(u - u_\ell)$$

$$v_t + u v_x + v v_y + p^{-1/\gamma} e^{\sigma} \frac{p_y}{\gamma} = -p^{-1/\gamma} e^{\sigma} Q\,v$$

$$\sigma_t + u\,\sigma_x + v\,\sigma_y = Q\left[\frac{1}{p} - p^{-1/\gamma} e^{\sigma} - \frac{\gamma-1}{2p}\left(2u_\ell u - u^2 - v^2\right)\right]$$

For the time being we have assumed that the velocity u_ℓ of the liquid propellants is undisturbed, which means that the droplet drag is vanishingly small. This produces a substantial simplification in the treatment because if the injection velocity is constant and axial, so the droplet velocity will remain at every location. Hence u_ℓ represents the constant value of the (axial) droplet velocity.

2.3 Steady-State Equations

Equations (1) can be applied, of course, also in steady state, or the corresponding solution can be obtained directly from the conservation equations written in finite form

$$\bar{p}^{-1/\gamma} e^{-\bar{\sigma}} \bar{u} = \bar{\rho}\bar{u} = \int_0^x \bar{Q}\,dx$$

$$\frac{\bar{p}-1}{\gamma} = \bar{p}^{-1/\gamma} e^{-\bar{\sigma}} \bar{u}\,(u_\ell - \bar{u}) = \bar{\rho}\,\bar{u}\,(u_\ell - \bar{u}) \qquad (1)$$

$$\bar{p}^{\frac{\gamma-1}{\gamma}} e^{\bar{\sigma}} = 1 - \frac{\gamma-1}{2}\,\bar{u}^2 = \frac{\bar{p}}{\bar{\rho}}$$

2.4 Purely Tangential Waves; First Order Equations

By definition the nondimensional values of steady-state pressure and temperature have been taken as unity at the injector and the corresponding sonic velocity has been used as reference velocity. Only two cases have been considered, the "purely" axial and the "purely" transversal cases. The purely axial case was developed by Mitchell, so here we will present only the transversal case. We assume that we have a spinning type of instability, traveling in the positive y direction. Then all quantities must be functions of

$$\alpha = ft - y$$

where f is the still unknown frequency. We see that any of the dependent variables must be periodic in α with period 1.

In the new variables the equations can be written

$$
\begin{aligned}
(f-v)\frac{p_\alpha}{\gamma} + u\,\frac{p_x}{\gamma} + p\,(u_x - v_\alpha) &= Q\left[1 - \frac{\gamma-1}{2}\left(2u_\ell u - u^2 - v^2\right)\right] \\
(f-v)\,u_\alpha + u\,u_x + p^{-1/\gamma} e^{\sigma}\,\frac{p_x}{\gamma} &= -p^{-1/\gamma} e^{\sigma}\,Q\,(u-u_\ell) \\
(f-v)\,v_\alpha + u\,v_x - p^{-1/\gamma} e^{\sigma}\,\frac{p_\alpha}{\gamma} &= -p^{-1/\gamma} e^{\sigma}\,Q\,v \\
(f-v)\,\sigma_\alpha + u\,\sigma_x &= Q\left[\frac{1}{p} - p^{-1/\gamma} e^{\sigma} - \frac{\gamma-1}{2p}\left(2u_\ell u - u^2 - v^2\right)\right]
\end{aligned}
\qquad (2)
$$

The boundary conditions at the injector and at the nozzle are at $x = 0$, $u = 0$ (3a)

$$\text{at} \quad x = \ell\,, \qquad M = \frac{u}{a} = \text{const.}\left(1 + \frac{\gamma-1}{2}\,\frac{u^2+v^2}{a^2}\right)^{\frac{1}{2}\,\frac{\gamma+1}{\gamma-1}} \qquad (3b)$$

where

$$a = (p/\rho)^{1/2} = p^{\frac{\gamma-1}{2\gamma}}\, e^{\sigma/2} \qquad (4)$$

represents the local sonic velocity. The nozzle boundary condition holds for a very short, multi-orifice nozzle, and was derived by Crocco and Sirignano.[14]

To these x-boundary conditions one has to add those of periodicity in the α variable. In the case where the spinning wave includes a shock, the conservation equations through the shock have also to be satisfied. We will expand all quantities in powers of a small parameter expressing the injection flux. Indeed, if the injection flux reduces to zero, the steady-state pressure becomes constant and uniform throughout the chamber. Hence any deviation from uniformity in space or from constancy in time should be related to the injection flux and vanish with it. Similarly, the axial velocity u reduces to zero if there is no combustion. Again both the steady value of u or its oscillations, or the oscillations of v and σ (their steady-state values are zero) should be related to the injection flux and vanish with it. Hence, calling μ the injection flux, we will assume the following expansions.

$$p = 1 + \mu p_1 + \mu^2 p_2 + O(\mu^3) \tag{5a}$$

$$u = \mu u_1 + \mu^2 u_2 + O(\mu^3) \tag{5b}$$

$$v = \mu v_1 + \mu^2 v_2 + O(\mu^3) \tag{5c}$$

$$\sigma = \mu \sigma_1 + \mu^2 \sigma_2 + O(\mu^3) \tag{5d}$$

$$Q = \mu Q_1 + \mu^2 Q_2 + O(\mu^3) \tag{5e}$$

We have taken $p_o = 1$ in agreement with the choice of the reference conditions for the steady-state solution.

The injection flux can be written as

$$\mu = \rho_{\ell i} u_\ell$$

where $\rho_{\ell i} = \rho_L A_i$ is the product of the actual liquid density times the injection port area A_i per unit area, and represents the actual droplet mass per unit chamber volume at injection. The injection flux, for a given propellant, can vary as a result of varying A_i and u_l. Here we shall assume that A_i is kept constant, in which case we can write

$$u_\ell = \mu u_{\ell 1} \qquad (\rho_{\ell i} u_{\ell 1} = 1) \tag{5f}$$

Observe that in steady state (assuming the combustion to be terminated before the nozzle entrance) we must have

$$\mu = \int_0^l \bar{Q}\, dx$$

Or, by virtue of Eq. (5e)

$$\int_0^l \bar{Q}_1\, dx = 1 \quad ; \quad \int_0^l \bar{Q}_2\, dx = 0 \quad ; \quad \dots \tag{6}$$

Insertion of the expressions (5) in the equations (2) will provide, after separation of the terms in different powers of μ, the equations to be solved. We notice that each one of equations (2) contains a mean convective term due to the steady-state gas velocity $\bar{u}$. The presence of the convective terms results in inconsistencies which we shall not discuss here, since they affect only terms in higher powers of μ than those considered in the present study. It is sufficient to say that the inconsistencies even in the higher order terms can probably be suppressed by using a double scale of axial length, according to a recently established technique for the treatment of certain nonlinear problems.

Another technique which is found useful in nonlinear problems is that of the coordinate stretching. Here we have already introduced a time stretching through the use of the frequency f, which can also be expanded as

$$f = 1 + \mu f_1 + \mu^2 f_2 + O(\mu^3) \tag{7}$$

where the constants f_1, f_2....... are to be determined and, of course, the frequency reduces to unity for $\mu = 0$.

In addition to this time stretching, it is convenient to introduce also a stretching of the variables α and x,* in the form of a series

$$\begin{aligned} \theta &= \alpha + \mu\,\theta_1(\theta, \xi) + \mu^2\theta_2(\theta, \xi) + O(\mu^3) \\ \xi &= x + \mu\,\xi_1(\theta, \xi) + \mu^2\xi_2(\theta, \xi) + O(\mu^3) \end{aligned} \tag{8}$$

*Observe that instead of introducing f, and stretching a and x, one could just stretch the original variables t, y, and x, with the same end results. The mixed procedure we are following here allows faster derivations.

where the functions θ_1, ξ_1, θ_2, ξ_2, ... are to be determined. All dependent variables are functions of θ, ξ; they must be periodic in θ with period 1. If there is a traveling transversal shock, we choose to stretch α in such a way that the shock corresponds to θ = const. In particular, if we place the shock at $\theta = 0$, because of the periodicity we must find again the shock at $\theta = 1$ and at any other integral value of θ.

The derivatives of a general quantity

$$F = F_0 + \mu F_1 + \mu^2 F_2 + O(\mu^3)$$

with F_o = const (as it is in all expansions (5)) can then be written as

$$F_\alpha = \mu F_{1\theta} + \mu^2 (F_{2\theta} + F_{1\theta}\theta_{1\theta} + F_{1\xi}\xi_{1\theta}) + O(\mu^3)$$

$$F_x = \mu F_{1\xi} + \mu^2 (F_{2\xi} + F_{1\theta}\theta_{1\xi} + F_{1\xi}\xi_{1\xi}) + O(\mu^3)$$

Introducing all the expansions above in Eq. (2) and separating the powers of μ we obtain the following equations for the first order quantities

$$\frac{p_{1\theta}}{\gamma} + u_{1\xi} - v_{1\theta} = Q_1 \tag{9a}$$

$$u_{1\theta} + \frac{p_{1\xi}}{\gamma} = 0 \tag{9b}$$

$$v_{1\theta} - \frac{p_{1\theta}}{\gamma} = 0 \tag{9c}$$

$$\sigma_{1\theta} = 0 \tag{9d}$$

2.5 Second Order Equations

The following are the second order equations :

$$\frac{p_{2\theta}}{\gamma} + \frac{p_{1\theta}}{\gamma}\theta_{1\theta} + \frac{p_{1\xi}}{\gamma}\xi_{1\theta} + (f_1 - v_1)\frac{p_{1\theta}}{\gamma} + u_1\frac{p_{1\xi}}{\gamma} + u_{2\xi} + u_{1\theta}\theta_{1\xi} + \tag{10a}$$

$$u_{1\xi}\xi_{1\xi} - v_{2\theta} - v_{1\theta}\theta_{1\theta} - v_{1\xi}\xi_{1\theta} + p_1(u_{1\xi} - v_{1\theta}) = Q_2$$

$$u_{2\theta} + u_{1\theta}\,\theta_{1\theta} + u_{1\xi}\,\xi_{1\theta} + (f_1 - v_1)\,u_{1\theta} + u_1\,u_{1\xi} + \frac{p_{2\xi}}{\gamma} + \frac{p_{1\theta}}{\gamma}\,\theta_{1\xi} + \tag{10b}$$
$$\frac{p_{1\xi}}{\gamma}\,\xi_{1\xi} - \left(\frac{p_1}{\gamma} - \sigma_1\right)\frac{p_{1\xi}}{\gamma} = -Q_1\,(u_1 - u_{\ell_1})$$

$$v_{2\theta} + v_{1\theta}\,\theta_{1\theta} + v_{1\xi}\,\xi_{1\theta} + (f_1 - v_1)\,v_{1\theta} + u_1 v_{1\xi} - \frac{p_{2\theta}}{\gamma} - \frac{p_{1\theta}}{\gamma} - \tag{10c}$$
$$\frac{p_{1\xi}}{\gamma}\,\xi_{1\theta} + \left(\frac{p_1}{\gamma} - \sigma_1\right)\frac{p_{1\theta}}{\gamma} = -Q_1\,v_1$$

$$\sigma_{2\theta} + \sigma_{1\theta}\,\theta_{1\theta} + \sigma_{1\xi}\,\xi_{1\theta} + (f_1 - v_1)\,\sigma_{1\theta} + u_1\,\sigma_{1\xi} = -Q_1\left(\frac{\gamma-1}{\gamma}\,p_1 + \sigma_1\right) \tag{10d}$$

The injector and nozzle conditions (3a) and (3b) are also expanded with the help of (4). They show that at the injector we must have

$$u_1'(\theta, 0) = u_2'(\theta, 0) = 0 \tag{11a}$$

and at the nozzle*

$$u_1'(\theta, \ell) = 0$$
$$u_2'(\theta,\ell) + u'_{1\xi}(\theta,\ell)\,\xi_1(\theta,\ell) = \bar{u}_1(\ell)\,a_1'(\theta,\ell) = \bar{u}_1(\ell)\left[\frac{\gamma-1}{2\gamma}\,p_1'(\theta,\ell) + \frac{\sigma_1'(\theta,\ell)}{2}\right] \tag{11b}$$

On the other hand, if there are shocks at $\theta = 0$ and 1 and we indicate with ΔF the jump of the quantity F through the shock, this is obviously a function of x only, and can be expanded as

$$\Delta F(x) = \mu\left[F_1(0,\xi) - F_1(1,\xi)\right]_{\xi=x} + \mu^2\left[F_2(0,\xi) - F_2(1,\xi) + \right.$$
$$\left.\xi_1(0,\xi)\,F_{1\xi}(0,\xi) - \xi_1(1,\xi)\,F_{1\xi}(1,\xi)\right]_{\xi=x} + O(\mu^3)$$
$$= \mu\,(\Delta F_1)_{\xi=x} + \mu^2\left(\Delta F_2 + \xi_{1m}\,\Delta F_{1\xi} + F_{1\xi m}\right)_{\xi=x} + O(\mu^3)$$

where we have defined for the general quantity $g(\theta, \xi)$ the two quantities

$$\Delta g = g(0,\xi) - g(1,\xi)$$
$$g_m = \frac{1}{2}\left[g(0,\xi) + g(1,\xi)\right]$$

*The assumption is made that combustion terminated at the nozzle entrance is steady state, so that $\bar{u}_{1\xi}(\ell) = 0$.

The equation of the shock located at $\Theta = 0$ is given by (8) as

$$\alpha = ft - y = -\mu\,\theta_1(0,\xi) - \mu^2\theta_2(0,\xi) + O(\mu^3) \tag{12a}$$

Hence the local angle between the shock and the axial direction is, to first order, given by

$$\beta = \left(\frac{dy}{dx}\right)_{t=const} = \mu\,\theta_{1\xi}(0,\xi) = \mu\,\beta_1 \tag{12b}$$

Applying the conservation equations through the shock one obtains the first and second order shock conditions in the form

$$\Delta u_1' = 0\ ;\quad \Delta\sigma_1' = 0\ ;\quad \Delta\left(v_1' - \frac{p_1'}{\gamma}\right) = 0 \tag{13}$$

$$\Delta u_2' + \xi_{1m}\Delta u_{1\xi}' + u_{1\xi m}\Delta\xi_1 = -\beta_1\Delta v_1'\ ;\quad \Delta\sigma_2' + \xi_{1m}\Delta\sigma_{1\xi}' + \sigma_{1\xi m}\Delta\xi_1 = 0$$

$$\Delta\left(v_2' - \frac{p_2'}{\gamma}\right) + \xi_{1m}\Delta\left(v_{1\xi}' - \frac{p_{1\xi}'}{\gamma}\right) + \left(v_{1\xi m}' - \frac{p_{1\xi m}'}{\gamma}\right)\Delta\xi_1 = \left(-\frac{\gamma+1}{2}p_{1m}' + \frac{\sigma_1'}{2}\right)\frac{\Delta p_1'}{\gamma} \tag{14}$$

The first equation of (13) and (14) represents the continuity of the tangential velocity component. The second equation in each group expresses that up to second order the shock is isentropic. The remaining equations express the invariance through the shock of the appropriate Riemann invariant $v - \frac{2}{\gamma-1}a$. This invariance holds indeed to second order for the oblique shock under consideration as for a normal shock. Observe that the second term of each Equation (14) vanishes because of Equations (13). Finally, it is evident that the shock velocity in the y direction is given by f. For the purposes of this treatment we need only the first order coefficient f_1 of the expansion (7). It is given by the same relation as if the shock were normal, and hence by the mean value of $v_1' + a_1'$ across the shock, that is by

$$f_1 = v_{1m}' + \frac{\gamma-1}{2\gamma}p_{1m}' + \frac{\sigma_1'}{2} \tag{15}$$

2.6 First Order Solution

The steady-state solution can be obtained either from Equations (9), setting all θ -derivatives equal to zero, or, more directly, from expansions of the Equation (1) already in finite form. The result is

$$\bar{u}_{1\xi} = \bar{Q}_1 \; ; \quad \bar{u}_1(\xi) = \int_0^{\xi} \bar{Q}_1 \, d\xi \; ; \quad \bar{p}_1 = \bar{\sigma}_1 = 0$$

Comparing with (6) we see that

$$\bar{u}_1(\ell) = 1 \tag{16}$$

For the unsteady components we obtain from Equation (9)

$$u'_{1\xi} = Q'_1 \; ; \quad \frac{p'_{1\xi}}{\gamma} = -u'_{1\theta} \; ; \quad v'_{1\theta} = \frac{p'_{1\theta}}{\gamma} \; ; \quad \sigma'_{1\theta} = 0 \tag{17}$$

For many combustion models (such as that considered later) the effect of the perturbed conditions on the combustion rate Q is not felt before the second order term Q_2'. Hence $Q_1' = 0$, and u_1'= const = 0 consistently with the injector and nozzle conditions (11a and b). This result is, of course, due to the assumption of purely transversal waves, as shown by the second Equation (17) which shows that p_1' must be a function of θ alone. Hence the other two equations (17) are satisfied by

$$v'_1 = \varphi(\theta) \; ; \quad \frac{p'_1}{\gamma} = \varphi(\theta) + C_1 \; ; \quad \sigma'_1 = C_2 \tag{18}$$

where C_1 and C_2 are constants to be determined,* and $\varphi(\theta)$ is an arbitrary function. It is clear that this solution satisfies the first order shock conditions (13).

2.7 Second Order Solution

The second order solution in steady state can again be obtained either from the Eq. (10) or directly from the Equation (1). If we assume $\bar{Q}(\xi) = \mu \, \bar{Q}_1(\xi)$ for all values of μ, then $\bar{Q}_2 = 0$, and one gets

$$\bar{u}_2 = 0 \; ; \quad \bar{p}_2 = \gamma \bar{u}_1 (u_{\ell_1} - \bar{u}_1) \; ; \quad \bar{\sigma}_2 = -(\gamma - 1)\bar{u}_1 \left(u_{\ell_1} - \frac{\bar{u}_1}{2}\right) \tag{19}$$

*Actually C_2 could be an arbitrary function of ξ, however, in the way C_1 and C_2 will be determined, it can be shown that C_2 is independent of ξ. For simplicity, we assume from the beginning that it is constant.

The equations for the unsteady components are then, using the relation $\bar{Q}_1(\xi) = \bar{u}_{1\xi}$

$$\frac{p'_{2\theta}}{\gamma} + u'_{2\xi} - v'_{2\theta} - \left[(\gamma+1)\varphi - f_1 + \gamma c_1\right]\varphi_\theta + \bar{u}_{1\xi}\left(\gamma\varphi + \gamma c_1 + \xi_{1\xi}\right) = Q'_2 \qquad (20a)$$

$$u'_{2\theta} + p'_{2\xi}/\gamma + \theta_{1\xi}\varphi_\theta + \bar{u}_{1\xi}\xi_{1\theta} = 0 \qquad (20b)$$

$$v'_{2\theta} - \frac{p'_{2\theta}}{\gamma} + (f_1 + c_1 - c_2)\varphi_\theta = -\bar{u}_{1\xi}\varphi \qquad (20c)$$

$$\sigma'_{2\theta} = -\bar{u}_{1\xi}\left[(\gamma-1)\varphi + (\gamma-1)c_1 + c_2\right] \qquad (20d)$$

2.8 Wave Shape Equation in the Most General Case

It is assumed that the constants c_1 and c_2 of Eq.(18) to be zero and this is generally the right value with some exceptions. We can then rewrite Eq. (18) so that:

$$v'_1 = \varphi(\theta) \quad ; \quad \frac{p'_1}{\gamma} = \varphi(\theta) \quad \text{and} \quad \sigma'_1 = 0 \qquad (21)$$

represent a possible first order solution (purely transverse wave). From Equation(15) we have (having taken $\xi_1 = 0$):

$$f_1 = \frac{\gamma+1}{2}\varphi_m$$

which results in the following equation

$$u'_{2\xi} - (\gamma+1)(\varphi - \varphi_m)\varphi_\theta + \bar{u}_{1\xi}(\gamma+1)\varphi = Q'_2 \qquad (22)$$

We also have:

$$u_{1\xi} = \bar{u}_{1\xi} = Q_1 = \bar{Q}_1 \qquad (23)$$

Multiplying Eq. (22) by μ^2 and Eq. (23) by μ, adding them up and recalling the expansions (5), we find the equation:

$$u_\xi = (\gamma+1)(v - v_m)v_\theta - \bar{u}_\xi(\gamma+1)v + Q$$

between the unexpanded quantities u, v, Q. This equation applies for the case when all quantities are periodic, and hence can be expressed as functions of θ = ft-y and ξ alone. If the solution is not periodic, every quantity should be considered to still depend on t, independently on the θ dependence. In this case an additional term should appear on the left hand side of the equation which writes:

$$u_\xi + 2v_t = (\gamma+1)(v - v_m)v_\theta - \bar{u}_\xi(\gamma+1)v + Q$$

In reality this equation holds only if $Q_1' = 0$, and if μ (and hence v) are small as well as when the Q perturbation is of order μ^2 while the steady state Q is of order μ. However, we shall suppose its approximate validity as well as that of Eq. (21) even in the case when Q' is of order μ, provided $v \ll 1$. Integrating from 0 to ℓ we obtain

$$u(\ell) = u_n = (\gamma+1)\ell(v - v_m)v_\theta - (\gamma+1)\bar{u}_n v + \int_0^\ell Q(\xi)\,d\xi$$

From the expanded nozzle condition, Eq. (11b), we can again (multiplying the first by μ and the second by μ^2 and adding up) synthesize the result:

$$u_n = \bar{u}_n\left(1 + \frac{\gamma-1}{2}v\right)$$

and hence we obtain:

$$(\gamma+1)\ell(v - v_m)v_\theta = \bar{u}_n\left(1 + \frac{3\gamma+1}{2}v\right) - \int_0^\ell Q(\xi)\,d\xi \qquad (24)$$

The corresponding equation in the non-periodic case is,

$$-2\ell v_t + (\gamma+1)\ell(v - v_m)v_\theta = \bar{u}_n\left(1 + \frac{3\gamma+1}{2}v\right) - \int_0^\ell Q(\xi)\,d\xi \qquad (24a)$$

When the relationship between Q and v is known, Equation (24) (or 24a) represents a nonlinear integro-differential equation for v.

2.9 Droplet Evaporation Model

The quasi-steady evaporation rate, under certain assumptions, is defined by the relation:

$$\frac{D_\ell r^*}{Dt^*} = \frac{\partial r^*}{\partial t^*} + u_\ell^* \frac{\partial r^*}{\partial x^*} = \frac{-K}{r^*}\left(1 + 0.3\, Re^{1/2}\, Pr^{1/3}\right)$$

where stars stand for dimensional quantities, K is a constant related to the properties of the gases and of the droplets, Pr is the Prandtl number, the Reynolds number is defined as:

$$Re = 2\,\frac{r^* \rho^* q^*_{rel}}{\mu^*}$$

and q^*_{rel} is the droplet velocity relative to the gas, given by:

$$q^{*2}_{rel} = (u^*_\ell - u^*)^2 + v^{*2}$$

Introducing the relative droplet volume

$$V = (r^*/r_i^*)^3$$

where r_i^* represents the droplet radius at injection, and non-dimensionalizing the other quantities in the usual fashion we obtain:

$$\frac{D_\ell V}{Dt} = f V_\alpha + u_\ell V_x = -C\left(V \rho\, q_{rel}\right)^{1/2} \qquad \text{(A)}$$

where we have: $$q^2_{rel} = (u_\ell - u)^2 + v^2$$

and $$C = \frac{0.9\sqrt{2}\, K \ell^* Pr^{1/3}}{c_r^* r_i^{*2}}\left(\frac{\rho_r^* r_i^* c_r^*}{\mu^*}\right)^{1/2}$$

contains the reference length ℓ^* (developed periphery of the annulus), the reference sonic velocity c_r^* and gas density ρ_r^* (in our case these are the corresponding values at the injector end) and the viscosity μ^* is the average gas viscosity.

The injection flux per unit area is given by:

$$\dot{m}_i^* = N^d \frac{4}{3}\pi r_i^{*3} \rho_L^* u_\ell^* = \rho_{\ell i}^*\, u_\ell^*$$

where N^d is the droplet number density which is constant since u_ℓ^* is constant, $\rho_L{}^*$ is the liquid propellant density, and $\rho_{\ell i}^*$ is the amount of propellant per unit chamber volume at injection. The dimensional evaporation rate is:

$$Q^* = -\mathcal{N}^d \frac{4}{3} \pi \rho_L^* \frac{D_\ell (r^{*3})}{Dt^*}$$

and its nondimensional value, $Q = \ell^* Q^* / \rho_r^* c_r^*$ is immediately proved to be:

$$Q = -\rho_{\ell i} \frac{D_\ell V}{Dt} \tag{B}$$

where $\rho_{\ell i} = \rho_{\ell i}^* / \rho_r^*$ is related to the nondimensional injection flux μ by the equation: $\mu = \rho_{\ell i} u_\ell$. Equations (A) and (B) completely define the source strength Q.

2.10 Wave Shape Equation With Droplet Evaporation Model

From Equations (A) and (B) we have:

$$-\frac{Q}{\rho_{\ell i}} = f V_\theta + u_\ell V_\xi = -c (V \rho\, q_{rel})^{1/2} \tag{25}$$

Here we have identified α with θ ($\theta_1 = 0$). Hence, taking $V^{\frac{1}{2}} = \nu$ we can write:

$$f \nu_\theta + u_\ell \nu_\xi = -\frac{c}{2} (\rho\, q_{rel})^{1/2} \tag{26}$$

Here: $$q_{rel}(\xi, \theta) = \left[(u_\ell - \bar{u})^2 + v^2 \right]^{1/2}$$

where u has been replaced by $\bar{u}$, consistently with the approximation that, to order μ , $u' = 0$, and where within the same accuracy, we can take (see Eq. (21))

$$f \simeq 1 + \mu f_1 \simeq 1 + \frac{\gamma+1}{2} v_m \; ; \; \rho \simeq 1 + \mu \frac{p_1'}{\gamma} \simeq 1 + v = \rho(\theta) \tag{27}$$

The formal solution $\nu(\xi, \theta)$ of Eq. (26) which has $\nu(0, \theta) = 1$ (initial droplet diameter fixed) is:

$$\nu(\xi, \theta) = 1 - \frac{c}{2u_\ell} \int_0^\xi \left[\rho\left(\theta - f \frac{\xi - \varsigma}{u_\ell}\right) q_{rel}\left(\varsigma, \theta - f \frac{\xi - \varsigma}{u_\ell}\right) \right]^{1/2} d\varsigma \tag{28}$$

after which Eq. (25) gives

$$Q(\xi,\theta) = \rho_{\ell i}\, C\left[\rho(\theta)\, q_{rel}(\xi,\theta)\right]^{1/2} \nu(\xi,\theta)$$

We have then Eq. (24) in the form:

$$(\gamma+1)\,\ell\,(v-v_m)\,v_\theta = \bar{u}_n\left(1+\frac{3\gamma+1}{2}v\right)-\rho_{\ell i}\, C\left[\rho(\theta)\right]^{1/2}\int_0^{\ell}\left[q_{rel}(\xi,\theta)\right]^{1/2}\nu(\xi,\theta)\,d\xi + 2\ell v_t \qquad (29)$$

the last term being present for non periodic solutions. Since Eq. (27) gives $\bar{\rho}=1$ (within the present approximation) we can obtain $\rho_{\ell i}$ from:

$$\mu = \rho_{\ell i}\, u_\ell = \bar{\rho}_n\, \bar{u}_n = \bar{u}_n \qquad (30)$$

The equation for v is now entirely defined for assigned values of C, $\bar{u}_n$, u_ℓ, γ and ℓ. It must be observed that it applies to the case of shock-type waves, and v_m represents the mean value at the shock with the frequency :

$$f = 1 + \frac{\gamma+1}{2}\, v_m$$

For shockless waves, of course, v_m is meaningless, but f is still meaningful, and v_m should be simply replaced by $(2/(\gamma+1))(f-1)$. In this case, instead of the unknown v_m to be determined simultaneously with the solution $v(\theta)$, we will have the unknown frequency f to be determined also in the same time as the solution $v(\theta)$.

We also have:

$$\bar{u} = \bar{u}_n\,(1-V) = \bar{u}_n\,(1-\bar{\nu}^2) \qquad (31)$$

Since $\bar{\rho} = 1$, and (30) $\mu = \bar{u}_n$. Hence we have from Eq. (26):

$$u_\ell\, \bar{\nu}_\xi = -\frac{C}{2}\left|u_\ell - \bar{u}\right|^{1/2} = -\frac{C}{2}\, u_\ell^{1/2}\left|1-\beta\,(1-\bar{\nu}^2)\right|^{1/2} \qquad (32)$$

where we have introduced $\beta = \bar{u}_n / u_\ell$

2.11 Case for $\beta < 1$

The solution of Equation (32) for $\beta < 1$, where $\bar{u} < u_\ell$ at all stations is:

$$\bar{\nu} = \left(\frac{1-\beta}{\beta}\right)^{1/2} \mathrm{Sh}\left[K\left(1-\frac{\delta}{\tau}\right)\right] \tag{33}$$

where

$$\delta = \frac{\xi}{u_\ell} \tag{34}$$

represents the time elapsed from the injection of the droplet,

$$\tau = \frac{b}{u_\ell} \tag{35}$$

is the droplet lifetime, b representing the station where, in steady state, $\bar{\nu} = 0$, and K being related to β by:

$$K(\beta) = \frac{1}{2} \ln \frac{1+\beta^{1/2}}{1-\beta^{1/2}} = \frac{1}{2} \ln \left|\frac{\beta^{1/2}+1}{\beta^{1/2}-1}\right|$$

The relation between b or τ and the constant c appearing in Eq. (25) is found to be:

$$c\, u_\ell^{1/2} \tau = \frac{c}{u_\ell^{1/2}} b = \frac{2K(\beta)}{\beta^{1/2}}$$

From Eqs. (31) and (32) we obtain then:

$$1 - \frac{\bar{u}}{u_\ell} = (1-\beta)\, \mathrm{Ch}^2\left[K\left(1-\frac{\delta}{\tau}\right)\right]$$

Application of Eq. (28) gives then:

$$\nu_1(\delta,\theta) = 1 - \frac{K}{\tau\beta^{1/2}} \int_0^{\delta} \left\{1+\frac{1}{2}v\left[\theta - f(\delta-\xi)\right]\right\}\left\{(1-\beta)^2 \mathrm{Ch}^4 K\left(1-\frac{\xi}{\tau}\right) + \frac{v^2}{u_\ell^2}\left[\theta - f(\delta-\xi)\right]^2\right\}^{1/4} d\xi \tag{36}$$

2.12 Case for $\beta > 1$

In the case $\beta > 1$, $\bar{u} < u_\ell$ only to a certain value of δ_* (or a certain station ξ_*, see Eq. (34)), where $\bar{\nu}$ becomes equal to a certain value $\bar{\nu}_*$; after this station we have $\bar{u} > u_\ell$.

We find for $\delta < \delta_*, \bar{\nu} > \bar{\nu}_*, \bar{u} < u_\ell$

$$\bar{\nu} = \bar{\nu}_* \, \mathrm{Ch}\left[K - (K + \pi/2)\frac{\delta}{\tau}\right]$$

$$1 - \frac{\bar{u}}{u_\ell} = (\beta - 1)\,\mathrm{Sh}^2\left[K - (K + \pi/2)\frac{\delta}{\tau}\right]$$

and for $\delta > \delta_*$, $\bar{\nu} < \bar{\nu}_*$, $\bar{u} > u_\ell$

$$\bar{\nu} = \bar{\nu}_* \cos\left[(K + \pi/2)\frac{\delta}{\tau} - K\right]$$

$$\frac{\bar{u}}{u_\ell} - 1 = (\beta - 1)\sin^2\left[(K + \pi/2)\frac{\delta}{\tau} - K\right]$$

with : $K(\beta) = \frac{1}{2}\ln\frac{\beta^{1/2}+1}{\beta^{1/2}-1} = \frac{1}{2}\ln\left|\frac{\beta^{1/2}+1}{\beta^{1/2}-1}\right|$

$$\bar{\nu}_* = \left(\frac{\beta - 1}{\beta}\right)^{1/2}$$

$$c\, u_\ell^{1/2}\tau = 2\int_0^1 \frac{d\bar{\nu}}{\left|1 - \beta(1 - \nu^2)\right|^{1/2}} = \frac{2}{\beta^{1/2}}(K + \pi/2)$$

$$\frac{\delta_*}{\tau} = \frac{K}{K + \pi/2}$$

For: $0 \leq \delta \leq \delta_*$ we have:

$$\nu_2(\delta,\theta) = 1 - \frac{K + \pi/2}{\tau\beta^{1/2}}\int_0^\delta \left\{(\beta-1)^2\,\mathrm{Sh}^4\left[K - (K + \pi/2)\frac{\xi}{\tau}\right] + \frac{1}{u_\ell^2}v^2\left[\theta - f(\delta - \xi)\right]\right\}^{1/4}\left\{1 + \frac{1}{2}v\left[\theta - f(\delta - \xi)\right]\right\} d\xi \tag{37}$$

and for $\delta > \delta_*$ we must take:

$$(\delta,\theta) = 1 - \frac{K+\pi/2}{\tau\,\beta^{1/2}}\left(\int_0^{\delta_*} \left\{ (\beta-1)^2\, Sh^4\left[K-\left(K+\frac{\pi}{2}\right)\frac{\xi}{\tau}\right] + \frac{1}{u_\ell^2}\,\upsilon^2\left[\theta - f(\delta-\xi)\right]\right\}^{1/4} \left\{1+\frac{1}{2}\upsilon\left[\theta - f(\delta-\xi)\right]\right\} d\xi \,+ \right.$$

$$\left. + \int_{\delta_*}^{\delta} \left\{ (\beta-1)^2 \sin^4\left[\left(K+\frac{\pi}{2}\right)\frac{\xi}{\tau} - K\right] + \frac{1}{u_\ell^2}\,\upsilon^2\left[\theta - f(\delta-\xi)\right]\right\}^{1/4} \left\{1+\frac{1}{2}\upsilon\left[\theta - f(\delta-\xi)\right]\right\} d\xi \right) \qquad (38)$$

Following Equation (27) we have taken: $\varrho^{1/2} \simeq 1 + \frac{1}{2}\upsilon$.

Finally we have all the elements to write the last term in Equation (29):

$$\varrho_{\ell_i}\, C\, \varrho^{1/2} \int_0^{\ell} \left[q_{rel}(\xi,\theta)\right]^{1/2} \nu(\xi,\theta)\, d\xi =$$

$$= \frac{2\beta^{1/2}K}{\tau}\, u_\ell \left[1+\frac{\upsilon(\theta)}{2}\right] \int_0^{\ell/u_\ell} \left[(1-\beta)^2\, Ch^4 K\left(1-\frac{\delta}{\tau}\right) + \frac{1}{u_\ell^2}\,\upsilon^2(\theta)\right]^{1/4} \nu_1(\delta,\theta)\, d\delta$$

for $\beta < 1$, and:

$$= 2\,\frac{\beta^{1/2}\left(K+\pi/2\right)}{\tau}\, u_\ell \left[1+\frac{\upsilon(\theta)}{2}\right]\left(\int_0^{\delta_*} \left\{(\beta-1)^2\, Sh^4\left[K-\left(K+\frac{\pi}{2}\right)\frac{\delta}{\tau}\right] + \frac{1}{u_\ell^2}\,\upsilon^2(\theta)\right\}^{1/4} \nu_2(\delta,\theta)\, d\delta \,+ \right.$$

$$\left. + \int_{\delta_*}^{\ell/u_\ell} \left\{(\beta-1)^2 \sin^4\left[\left(K+\frac{\pi}{2}\right)\frac{\delta}{\tau} - K\right] + \frac{1}{u_\ell^2}\,\upsilon^2(\theta)\right\}^{1/4} \nu_3(\delta,\theta)\, d\delta \right)$$

for $\beta > 1$.

It is obvious that any negative value of ν resulting from Equation (36) or (38) must be replaced by 0 .

SECTION III

Numerical Analysis for Periodic Solutions

This section concerns the numerical integration of the wave equation [Eq. (29)] in the previous section. A shock-type solution is sought in the case of $\partial v/\partial t = 0$ which represents the case of a periodic solution. It is useful to recall that in a linear treatment once instability appears, the amplitude of the perturbation grows indefinitely larger with time. Of course, in reality, this is not so, because of the presence of nonlinear effects resulting in a limitation of the final amplitude.

Crocco's mathematical study of the nonlinear behavior in the case of a thin annular chamber has, indeed, the purpose of determining the limiting-cycle (periodic solution) of a linearly unstable rocket. However, an even more useful goal is the solution of the problem of nonlinear instability, that is instability which may result during an otherwise stable run, when the application of disturbances of a sufficiently high level results in amplification, while disturbances of lower-level decay. This kind of instability is said to be "triggering instability" and the corresponding "threshold" has a periodic solution which is called "triggering cycle". For this kind of analysis it is immaterial if $\beta < 1$ or $\beta > 1$.

3.1 Solution of the Nonlinear Integral-Differential Equation (29)

If the integral appearing in the last term of Eq. (29) is formally reduced to a simple function $M(\Theta)$, the same equation may be written as follows:

$$(\gamma+1)\ell\,(v - v_m)\,v_\theta = \bar{u}_n\left[1 + \frac{3\gamma+1}{2}v(\theta)\right] - \frac{2\beta^{1/2}K}{\tau}\,u_\ell\left[1 + \frac{v(\theta)}{2}\right]M(\theta) \qquad (39)$$

adding further simplifications,

$$(v - v_m)\,v_\theta = A + B\,v(\theta) - D\left[1 + \frac{v(\theta)}{2}\right]M(\theta) \qquad (40)$$

where

$$A = \frac{\bar{u}_n}{(\gamma+1)\ell} \; ; \quad B = \frac{(3\gamma+1)}{2(\gamma+1)} \frac{\bar{u}_n}{\ell} \; ; \quad D = \frac{2\beta^{1/2} K u_e}{\tau(\gamma+1)\ell} \tag{41}$$

are constants for given: $\gamma, \ell, u_\ell, \bar{u}_n$ (and hence β), and b (or $\tau = \frac{b}{u_\ell}$).

Let us define the right-hand side of Eq. (4) as g(θ), where g is seen to be a linear integral function. With this assumption, Eq. (40) may be written:

$$(v - v_m)\, v_\theta = g(\theta) \tag{42}$$

or:

$$v_\theta = \frac{g(\theta)}{v - v_m} \tag{43}$$

where:

$$v_m = \frac{1}{2}\left[v(0) + v(1)\right] \tag{44}$$

Since we have a periodic solution with discontinuities only at the endpoints of the interval $0 \leq \theta \leq 1$, it follows that there is some θ * in this range, such that $v(\theta^*) = v_m$. From Eq. (43) it is seen that θ * is a singular point and for that equation to have meaning it must be:

$$g(\theta^*) = 0 \tag{45}$$

Integration of Eq. (42) yields the formal relation

$$\left[v(\theta) - v_m\right]^2 = \left[v(0) - v_m\right]^2 + 2\int_0^\theta g(\theta')\, d\theta' \tag{46}$$

Evaluation of Eq. (46) at $\theta = 1$ and the definition Eq. (45) combine to yield another condition on the function g (θ), namely:

$$\int_0^1 g(\theta)\, d\theta = 0 \tag{47}$$

Equation (21) may be considered as a quadratic relation for $g(\theta)$ and, therefore, has two solutions. It may readily be seen that, in the case where a shock exists and so $v(1) \neq v(0)$ we must have:

$$v(\theta) = v_m + \left\{ \left[v(0) - v_m \right]^2 + 2 \int_0^{\theta} g \, d\theta' \right\}^{1/2} \tag{48a}$$

for $0 \leq \theta \leq \theta^*$, and

$$v(\theta) = v_m - \left\{ \left[v(0) - v_m \right]^2 + 2 \int_0^{\theta} g \, d\theta' \right\}^{1/2} \tag{48b}$$

for $\theta^* \leq \theta \leq 1$.

In the particular case which arises for $\theta = \theta^*$, $v(\theta^*) = v_m$ and so Eqs. (48) yield:

$$\left\{ \left[v(0) - v_m \right]^2 + 2 \int_0^{\theta^*} g \, d\theta' \right\}^{1/2} = 0 \tag{49}$$

In order to obtain real-valued solutions that are continuous at θ^*, it is necessary that (let us call $G(\theta) = \int_0^{\theta} g \, d\theta'$):

$$G(\theta^*) = \int_0^{\theta^*} g \, d\theta'$$

has a certain negative value such that the term under the square-root sign in Eq. (48) has a local minimum value (which equals zero) at $\theta = \theta^*$. This is consistent with the fact that $g = 0$ at $\theta = \theta^*$.

From Eq. (49) it follows:

$$v_m = v(0) - \sqrt{-2G(\theta^*)} \tag{50}$$

Of course, Eq. (48) is merely an implicit relation for $v(\theta)$, since $g(\theta)$ depends upon $v(\theta)$; however, the equation is in convenient form to solve by Picard's method.

The iteration procedure used begins with assuming $\upsilon(\theta) = \upsilon(0) + \phi(\theta)$ where $\phi(0) = 0$. An initial guess of $\phi(\theta)$ is made (typically, a sawtooth profile was assumed), but rather than specifying $\upsilon(0)$, Eq. (47) is used to calculate $\upsilon(0)$.

Knowing $\upsilon(0)$ and $\phi(\theta)$, $\upsilon(\theta)$ is immediately known and may be substituted into the right-hand side of Eq. (48). Then use is made of Condition (45) for which Eq. (49) is true and by means of Eq. (50), υ_m may be determined. Eq. (48) is then used to calculate a new $\upsilon(\theta)$. Subtracting $\upsilon(0)$ from $\upsilon(\theta)$, a new $\phi(\theta)$ is known and then Eq. (48) is again used to calculate a new $\upsilon(0)$ and so forth, until the sequences for $\upsilon(\theta)$ and υ_m converge.

The iteration was performed on an IBM 360/91 computer with the solutions converging in approximately ten to fifteen steps. In all the cases where different initial profiles for $\phi(\theta)$ were assumed, the same limiting solution was obtained. Usually the qualitative behavior is demonstrated immediately (in the case of convergence) by the first step in the iterative procedure.

3.2 Influence of β Upon the Numerical Analysis

As it was stated at the beginning of Section III, it is immaterial whether β is > 1 or < 1 as far as the iteration method is concerned. Only the function $M(\theta)$ is affected because it takes on two different forms according to the value of β compared to 1. For $\beta > 1$, a station δ_* exists in the combustion chamber where the gas velocity gets larger than u_ℓ. This is because at the nozzle entrance $\bar{u}_h > u_\ell$ and thus the way to calculate ν is split in two parts as shown in Eq. (38).

For information, the computer program for $\beta > 1$ has been introduced in Appendix A. The reason is that the situation $\beta > 1$ is more likely to occur in reality and another reason is that its numerical generality makes the case $\beta < 1$ a special case.

3.3 Discussion of Results for Periodic Solutions

One of the most interesting and important conclusions that can be drawn from the numerical solution of Eq. (29) for $\frac{\partial v}{\partial t} = v_t = 0$ is that a shock-type pressure distribution does exist within the annular chamber.

Depending on the magnitude of the gas velocity at the nozzle entrance compared to the constant droplet velocity (i.e., depending on whether $\beta = \bar{u}_n / u_\ell$ is $\lessgtr 1$) we can have a shock-type pressure distribution as shown in Fig. 2 or in Fig. 3. In both cases the wave decays sharply at the beginning (low values of θ) or, as to say, decays for high negative values of $d\sigma / d\theta$, especially for the case $\beta > 1$ for which larger amplitudes exist also as a general result.

The characteristic droplet lifetime τ , in the way it is defined by Eq. (35) (time elapsed from the injection of the droplet to the moment it vanishes) influences the shock amplitude and, in a more sensitive way, the energy associated with it as it will be seen later.

Fig. 4 shows how wave amplitudes are distributed for given combustion chamber length and droplet velocity for various values of τ . The wave shape for $\tau = 0.8$ is significant of a situation where for smaller values of τ the convergence towards the solution becomes more difficult to obtain until the situation is reached where no solutions exist in the sense that no convergence is obtained in the numerical iteration procedure.

The periodic solution is a condition of dynamic equilibrium and, as such, may be stable or unstable. If the amplitude is perturbed slightly from the value for a periodic solution, the perturbation may grow or decay. If both positive and negative perturbations grow in absolute magnitude, the periodic solution is unstable (triggering cycle) while if both positive and negative perturbations decay, the periodic solution is stable (limiting cycle). We are not in a position to assert that the periodic solution we obtained is the triggering cycle, and it is likely to be such, because of small wave amplitudes involved, etc. A systematic search has been performed in order to find the limiting cycle for given values of l, u_1, β and position at which droplets vanish (actually the parameters were l = 0.40, u_1 = 0.10, b = 50%, β = 1.1 and the initial wave amplitude guess was of 0(40), which means of the order of 200 times more than the triggering cycle amplitude). From such an initial high value of the wave amplitude all the following wave amplitudes, during the iteration procedure, converged to lower and lower amplitudes, reaching the triggering cycle without being "caught" by any other solution. A third order, highly involved mathematical analysis, could perhaps yield a limiting cycle which certainly exists for $t \rightarrow \infty$.

A comparison can be made with Crocco's previous calculations, where the results are valid only for $v \ll u_\ell$ and for $\bar{u} \ll u_\ell$ and no chance is given for $\bar{u}$ to become larger than u_ℓ, as is the case in the present work where we have $\beta > 1$. There it is shown that a shock-type solution can appear only if $\ell u_{\ell 1}^2 \leq 1/33.8$, i.e., only if $\beta \geq 33.8$ (in fact $u_{\ell 1} = u_\ell / \mu^{1/2} = u_\ell / \bar{u}_n^{1/2}$). Actually this condition is quite well satisfied in the present case as long as β is small; it is possible to show that Eq. (29) yields the same conclusions mentioned above as long as $\beta \rightarrow 0$ and numerical computations have shown that it is no longer possible to obtain solutions for $\beta < 0.15$ ($\ell = 0.15$ and $u_\ell = 0.02$ have been taken).

From Figures 2 and 3 it is easy to compare the breadth of the wave profile in the two cases where the gas velocity at the nozzle entrance is smaller than u_ℓ (β = 0.8) and larger than u_ℓ (β = 1.1). The more β increases, the more the wave amplitude increases (for β = 5, the value of p/γ = v(0) (at θ = 0) reaches 0.46). The most significant way to look at the behavior of the shock-type pressure distribution is by studying the behavior of the energy associated with the wave, versus the droplet characteristic lifetime τ. In this study we are considering the case of a spinning wave and the energy $\mathcal{E}$ associated with it (kinetic energy + potential energy) that is proportional to $\int_0^1 v^2 d\theta = \int_0^1 (p/\gamma)^2 d\theta$. Figures 5 and 6 show the behavior of $\mathcal{E}$ versus τ for β = 0.8 and for β = 1.1 and in each case for given ℓ and u_ℓ.

The parameter τ has been made variable by changing the combustion distribution length (station b at which droplets vanish) and keeping ℓ and u_ℓ constant. Considering that the energy associated with the triggering cycle should be minimum where the instability is most likely to happen, (because more energy should be put in the wave in order to drive the instability), such a condition is not reached for $\beta = 0.8$, Fig. 5 (note that the curve is smoother for $\tau = 0.5$). A common feature appears evident from Figures 5 and 6; the effect of τ upon the energy $\mathcal{E}$ gets less and less evident as long as τ increases consistent with Crocco's previous calculations For $\beta = 1.1$, as it is shown in Fig. 6, the instability is more likely to occur for values of τ ranging from 0.5 to 1.2 (from $\ell = 0.2$ to $\ell = 0.4$). Numerical computations have shown that, at least for $u_\ell = 0.1$, and for values of ℓ close to 0.3, it is easier to obtain solutions for $\beta > 1$ than for $\beta < 1$. This, perhaps, is the reason why we could not reach a minimum for $\mathcal{E}$ in the case of $\beta = 0.8$. A discontinuity appears for $\tau = 1.4$, but on the ground of theoretical analysis no singularity appears in Eq. (29) to give a justification and besides pressure distributions for values of τ in the neighborhood of the discontinuity appear to be normally behaved. Nevertheless, convergence is reached faster, for $\beta < 1$ when ℓ, as well as u_ℓ, are given lower values.

Figure 7 shows that the energy associated with the triggering cycle (everything being equal) becomes smaller when the droplet velocity increases and that it is influenced in lesser extent by τ.

A common characteristic appears from Figure 6 and that is for values of τ lower than $\tau_{\mathcal{E}_{min}}$ (value of τ for which $\mathcal{E}$ is minimum) the tendency towards instability becomes increasingly high and at a very fast rate, up to a point where no valid solutions are obtained (dotted portions of curves for ℓ = constant).

Crocco and Mitchell[15] in their theoretical investigation on the transverse combustion instability for an annular motor, used the n- τ model and in doing so they expressed the second order combustion rate Q'_2 as follows:

$$Q'_2(\xi,\theta) = n\,\bar{u}_{1\xi}(\xi)\left[p'_1(\xi,\theta) - p'_1(\xi,\theta-\tilde{\tau})\right] \tag{51}$$

where n is the interaction index, $\tilde{\tau}$ the stretched time lag and $\theta-\tilde{\tau}$ a retarded variable.

In the present work the instantaneous combustion rate is related to other physical factors such as the droplet relative volume, the gas density and the gas relative velocity, as can be seen from Eq. (25). From Crocco's time lag theory we can assume that the physical factors are correlated and we can disregard the explicit effects of all the factors except that of the pressure and say that the rate of combustion and pressure are related together by means of the interaction index n. Under this assumption we can say that a given local and instantaneous combustion rate, at any value of the interaction index n, corresponds to a pressure disturbance p. Through the integration $\int_0^1 (p/\gamma)^2 d\theta$ we can say, from the present work, that we still have two values of τ for any ξ in the region of $\xi_{minimum}$.

SECTION IV

CONCLUSIONS

The theoretical work described in this report provides conformation to the experimental observations of Harrje, Varma and others that shock-type waves are characteristic of transverse mode instability in an annular chamber.

The following is a listing of the practical considerations that one can derive from this theoretical investigation of an annular rocket motor experiencing first tangential mode combustion instability.

1) For the more realistic case of $\beta = \bar{u}_n/u_\ell > 1$ (since the gas velocity at the nozzle entrance is most likely to be larger than the liquid propellant velocity) Fig. 6 shows that in the particular case of $\beta = 1.1$ and $u_\ell = 0.10$ a combustion distribution extending to approximately 30% of the chamber length must be avoided. With such a combustion concentration, the energy feedback required to trigger combustion instability is minimized. The behavior of the energy for different values of β has not been investigated.

2) Figure 6 also shows that for a combustion distribution below 20-25% of the combustion chamber length no shock-type instability can be triggered. This would appear to indicate that these combustion lengths represent the best point to complete combustion. If the combustion distribution is required to be spread further along the chamber axis, then Fig. 6 shows that it is far better to attempt to provide very large values of τ (characteristic time required for a complete combustion). This takes advantage of the higher energies required for triggering the instability with large τ and thereby moves the operational point further from the limits of unstable combustion.

3) Again from Fig. 6 it is shown that improved stability is achieved if the combustion chamber length is taken as small as possible compared to the mean circumference of the annulus (for example, $\ell = \ell^*/\pi d^* = 0.33$ represents the length of a square

longitudinal cross section combustion chamber, i.e., where $\ell^* = d$, here d^* is the dimensional mean diameter of the annulus). For large values of τ it is far more convenient to operate with a short combustion chamber, since a larger quantity of feedback energy is then required (i.e., more stable operation).

4) It is also suggested to operate at as low an injection velocity as possible in order to increase the feedback energy required for triggering the instability. This trend is shown by Fig. 7 where for $\beta = 1.1$ and $\ell = 0.3$ larger energy requirements for instability are associated with $u_\ell = 0.10$ than with $u_\ell = 0.12$. Actually, the parameters u_ℓ, b and ℓ are not completely independent, because of the effect of u_ℓ on the combustion distribution.

5) For a given injection velocity and chamber length, another way to stabilize an engine (i.e., require more energy to drive the instability) is by increasing β which means making the gas velocity at the nozzle entrance as large as possible compared to the liquid injection velocity. This is shown by Figs. 5 and 6 for a transition from $\beta = 0.8$ to $\beta = 1.1$, where shock amplitudes and associated energies become larger and larger (for $\beta = 5$, $P'_{1/\gamma} = 0.46$) enlarging the safety margin from the instability limit. Likewise, as has been pointed out above, the increasing of β by increasing the gas velocity at the nozzle entrance would also affect other parameters which in this specific case have been taken as constant. It should be pointed out that in this theoretical investigation the energy associated with the shock wave has been considered per unit volume of the combustion chamber. If, on the other hand, energy computations for the <u>overall</u> combustion chamber volume are made, that situation would lead towards reversing the relative position of the curves, i.e., the longer chamber with more volume would exhibit the larger overall energy levels (Fig. 6).

To summarize the design requirements needed to operate as far as possible from the triggering limit one should (apart from requiring solutions such as baffles and acoustic liners):

a) Either distribute the combustion over a range not exceeding

20% of the combustion chamber length, or spread the combustion over the entire length of the combustion chamber (this is to avoid the minimum energy zone of 30% of the combustion length).

b) Keep the combustion chamber length as small as possible compared to the mean annulus circumference (πd^*).

c) Maximize β by injecting the liquid propellant at the lowest velocity and maintaining the gas velocity at the nozzle entrance as high as possible.

REFERENCES

1. Crocco, L. and Cheng, S. I., "Theory of Combustion Instability in Liquid Propellant Rocket Motors", AGARDOgraph No. 8, Butterworths Scientific Pub., LTD., London, 1956.

2. Gunder, D. F. and Friant, D. R., "Stability of Flow in a Rocket Motor", Journal of Applied Mechanics, Vol. 17, p. 327 (1950).

3. Yachter, M., "Discussion of the paper of Ref 2, "Journal Applied Mechanics, Vol. 18, p. 114 (1951).

4. Summerfield, M., "A Theory of Unstable Combustion in Liquid Propellant Rocket Systems", Journal American Rocket Society, Vol. 21, p. 108 (1951).

5. Ellis, H., Odgers, I., Stosick, A. J., Van de Verg, N. and Wick, R. S., "Experimental Investigations of Combustion Instability in Rocket Motors", Fourth Symposium on Combustion, Williams and Wilkins Co., 1953.

6. Scala, S. M., "Transverse Wave and Entropy Wave Combustion Instability in Liquid Propellant Rockets", Princeton University, Ph.D. Thesis, Aero. Engineering Report No. 380, April 1, 1957.

7. Osborn, J. R. and Bonnell, J. M., "On the Importance of Combustion Chamber Geometry in High Frequency Oscillations in Rocket Motors", Paper presented at the ARS Semi-Annual Meeting, Los Angeles, Cal., May 9-12, 1960.

8. Crocco, L., Grey, J. and Harrje, D. T., "Theory of Liquid Propellant Rocket Combustion Instability and Its Experimental Verification", ARS Journal, Vol. 30, No. 2, February, 1960.

9. Priem, R. J. and Guentert, D. C., "Combustion Instability Limits Determined by a Nonlinear Theory and a One-Dimensional Model", NASA TN D-1409, Oct. 1962.

10. Sirignano, W. A., "A Theoretical Study of Nonlinear Combustion Instability: Longitudinal Mode", Technical Report No. 677, Dept. of Aerospace and Mech. Sciences, Princeton University, March 1964 (Ph.D. Thesis).

11. Crocco, L., "Research on Combustion Instability in Liquid Propellant Rockets", XII Symposium (International) on Combustion, pp. 85-99, 1969.

12. Crocco, L., "Theoretical Studies on Liquid Propellant Rocket Instability", Tenth Symposium (International) on Combustion, pp. 1101-1128, 1965.

13. Priem, R. J. and Heidmann, M. F., "Propellant Vaporization as a Design Criterion for Rocket Engine Combustion Chambers", NASA TR R-67, 1960.

14. Crocco L., and Sirignano W. A., "Effect of the Transverse Velocity Component of the Nonlinear Behavior of Short Nozzles", AIAA Journal, Vol. 4, No. 8, 1966.

15. Crocco, L., Mitchell, C. E., "Nonlinear Periodic Oscillations in Rocket Motors with Distributed Combustion", Combustion Science and Technology, Vol. 1, No. 2, Sept. 1969, pp. 147-169.

APPENDIX A
Computer Program for Periodic Solution with $\beta > 1$

```
FORTRAN IV G LEVEL  19                MAIN                DATE = 71053          21/52/00

0001          DIMENSION F(200),G(200),Q(200),FT(200),ET(200),FINE(200),DIF(200),
             1FINE(200),TIC(200),PSI(200),V(200),CAPG(200),SMALLG(200),V1(200),
             1Q1(200),Q2(200),Q3(200),CRI(200),V2(200),V1SQ(200)
0002          READ(5,10) JDELT,ITETA,JVNB,S,VK,BE,UL,PCNT,VINT,EN
0003       10 FORMAT(3I4,6F10.5,F8.3)
0004          READ(5,14) CCEF,DVSN
0005       14 FORMAT(2F10.5)
0006          READ(5,500) (PSI(K3),K3=1,21)
0007      500 FORMAT(7(2X,F8.0),10X)
0008          WRITE(6,247) EN,COEF,DVSN
0009      247 FORMAT(/30X,6H EN = ,F10.4,8H COEF = ,F10.4,8H DVSN = ,F10.4/)
0010          WRITE(6,20)JDELT,ITETA,JVNB,S,VK,BF,UL,PCNT
0011       20 FORMAT(10H DELTAS = ,I4,9H TETAS = ,I4,9H VK(0) = ,I4,5H L = ,
             1F7.4,15H FIRST VK(0) = ,F9.4,8H BETA = ,F7.4,
             16H UL = ,F7.4,5H B = ,F7.4)
0012          WRITE(6,22)VINT
0013       22 FORMAT(15H DELTA VK(0) = ,F9.4)
0014          VKAPPA=VK
0015          CA=0.5*ALOG(ABS((BE**0.5+1.0)/(BE**0.5-1.0)))
0016          TAU=PCNT*S/UL
0017          R=S/UL
0018          PAI=3.141592
0019          RAT=((BE**0.5)*TAU)/(2.0*(CA+PAI*0.5))
0020          AC=(BE*UL)/(2.2*S)
0021          BC=(BE*UL)*1.044/S
0022          DC=(2.0*(BE**0.5)*(CA+PAI*0.5)*UL)/(TAU*2.2*S)
0023          DLTSTR=TAU*CA/(CA+0.5*PAI)
0024          WRITE(6,23) AC,BC,DC,DLTSTR
0025       23 FORMAT(10X,5H A = ,F7.4,5H B = ,F7.4,5H D = ,F7.4,10H DLTSTR = ,F7
             1.4)
0026          WRITE(6,25) CA,TAU,R,RAT
0027       25 FORMAT(11H K(BETA) = ,1PE12.4,7H TAU = ,1PE12.4,
             18H L/UL = ,1PE12.4,7H RAT = ,1PE12.4)
0028          TETA=ITETA
0029          DTETA=1.0/TETA
0030          ITETP=ITETA+1
0031          DELT=JDELT
0032          DDELT=R/DELT
0033          JDELP=JDELT+1
0034          LAPPA=2
0035          LAST=1
0036       15 MARY=1
0037          VKINT=0.10*VK
0038          MINA=1
0039          LIRA=1
0040          LAMA=1
0041          MAMA=1
0042          MELA=1
0043          LUNA=ITETP
0044       26 DO 800 I=1,JVNB
0045          WRITE(6,12) VK
0046       12 FORMAT(/10H VK(0)I = ,F12.7)
0047       24  GO TO (27,11),MAMA
0048       27 TI=0.0
0049          KLV=1
0050       11 DO 700 K3=KLV,ITETP
```

```
   13 DJ=0.0
      DO 620 K2=1,JDELP
      GO TO (284,286),LAPPA
  284 FRK=1.0+1.1*(VK-0.5*COEF)
      GO TO 1416
  286 FRK=1.0+1.1*(VK+0.5*PSI(ITETP))
 1416 MAGGIO=1
      MAGGIO=1
      LAFIN=1
      LIMBO=1
      IF(DJ.GT.DLTSTR) GO TO 41
   40 A=TI-FRK*DJ
      KOV=1
      GO TO 42
   41 DJMDST=DJ-DLTSTR
      IF(DJMDST.LT.DDELT) GO TO 64
  203 A=TI-FRK*DJMDST
      MISA=1
      KOV=2
      LAFIN=2
      GO TO 66
   64 LIRSTK=K2
      SECT=DJMDST
      LASTK=LIRSTK-1
      IF(LASTK.LT.3) GO TO 242
      GO TO 243
  242 WRITE(6,244)
  244 FORMAT(2X,14H LASTK IS LT 3)
      STOP
  243 BEBE=DJ
      A=TI-FRK*DLTSTR
      DJ=DLTSTR
   66 GO TO (45,46), LAFIN
   45 MAGGIO=2
      GO TO 42
   46 MAGGIO=3
      LIMBO=2
      GO TO 42
   42 J=A
  251 B=J
      EI=A
      BI=B
      D=B-A
      IAC=1
      IF(D) 50,60,100
   50 IF((A.GT.0.0).AND.(A.LT.1.0)) GO TO 110
      ALFA=B
      GO TO 30
   60 IF(A) 70,80,90
   70 ALFA=B
      B=B+1.0
      GO TO 30
   80 ALFA=0.0
      B=TI
      GO TO 30
   90 IF(A.NE.1.0) GO TO 98
```

```
   92 ALFA=0.0
      B=TI
      GO TO 30
   98 ALFA=B-1.0
      B=B-1.0
      GO TO 30
  100 ALFA=B-1.0
      GO TO 30
  110 ALFA=0.0
      E=TI-A
      IF(E) 120,130,140
  120 B=TI
      GO TO 30
  130 ANU1=1.0
      MONA=1
      GO TO 600
  140 B=TI
   30 DX=(B-A)/20.0
      DDX=ABS(DX)
      X=A
      DO 180 L=1,21
      CSI=X-ALFA
      GO TO (392,393),LAPPA
  392 FUN=COEF*(2.0*(CSI**EN)-EN*(CSI**2))/(EN-2.0)
      GO TO 290
  393 TITTI=0.0
      DO 334 IL=1,LUNA
      IF(IL.EQ.1) GO TO 332
      ILM=IL-1
      TITTIM=TITTI-DTETA
  336 IF(CSI.GE.TITTI) GO TO 332
      FUN=PSI(ILM)+(CSI-TITTIM)*(PSI(IL)-PSI(ILM))/DTETA
      GO TO 290
  332 TITTI=TITTI+DTETA
  334 CONTINUE
  290 GO TO(335,48), LIMBO
  335 F(L)=(1.0+0.5*(VK+FUN))*(((BE-1.0)**2)*(SINH(CA-(CA+0.5*PAI)
     1*(DJ*FRK-(TI-X))/(FRK*TAU)))**4+((VK+FUN)/UL)**2)**0.25
      LOVA=1
      GO TO 52
   48 F(L)=(1.0+0.5*(VK+FUN))*(((BE-1.0)**2)*(SIN((CA+0.5*PAI)*(DJ*FRK-(
     1TI-X))/(FRK*TAU)-CA)**4)+((VK+FUN)/UL)**2)**0.25
      LOVA=2
   52 X=X+DX
  180 CONTINUE
      NSEGAP=21
  190 CALL QSF(DDX,F,G,NSEGAP)
      IF((EI.GE.0.0).AND.(EI.LE.1.0)) GO TO 400
      GO TO (195,210,220,230),IAC
  195 AINT=G(NSEGAP)
  200 ALFA=0.0
      A=0.0
      B=1.0
      IAC=2
      GO TO 30
  210 PER=G(NSEGAP)
```

```
      IF(EI.LT.0.0) GO TO 225
      BINT=(BI-1.0)*PER
      IAC=3
      A=1.0
      GO TO 92
  220 ANU1=1.0-((CA+0.5*PAI)/(FRK*TAU*(BE**0.5)))*(AINT+BINT+G(NSEGAP))
      MONA=2
      GO TO 600
  225 BINT=ABS(BI)*PER
      IAC=4
      A=0.0
      GO TO 80
  230 GO TO 220
  400 GO TO 231
  231 ANU1=1.0-((CA+0.5*PAI)/(FRK*TAU*(BE**0.5)))*G(NSEGAP)
      MONA=3
      GO TO (350,351),LAPPA
  350 RUN=COEF*(2.0*(TI**EN)-EN*(TI**2))/(EN-2.0)
      GO TO 600
  351 RUN=PSI(K3)
  600 GO TO (43,16,47), MAGGIO
   43 IF(DJ.GT.DLTSTR) GO TO 609
   16 Q1(K2)=((((BE-1.0)**2)*(SINH(CA-(CA+0.5*PAI)*DJ/TAU))**4+
     1((VK+RUN)/UL)**2)**0.25)*ANU1
      Q1STR=Q1(K2)
  252 IF((DJ-DLTSTR).EQ.0.0) GO TO 245
      GO TO 209
  245 CINTST=1.0-ANU1
      ANUSTR=ANU1
      STAR2 =((((BE-1.0)**2)*(SIN(((CA+0.5*PAI)*DJ/TAU)-CA))**4+
     1 ((VK+RUN)/UL)**2)**0.25)*ANUSTR
      MISA=2
      DJ=BEBE
  209 IF(Q1(K2).LT.0.0) GO TO 249
      GO TO 609
  249 JL=K2-1
      IF(JL.EQ.1) GO TO 228
      GO TO 227
  228 G(JL)=0.0
      GO TO 226
  227 IF(JL.EQ.2) GO TO 224
      GO TO 223
  224 JLM=JL-1
      G(JL)=(Q1(JLM)+Q1(JL))*DDELT*0.5
      GO TO 226
  223 CALL QSF(DDELT,Q1,G,JL)
  226 D1=DJ-DDELT
      Z1=((D1)*Q1(K2)-DJ*Q1(JL))/(Q1(K2)-Q1(JL))
      ATRI1=0.5*(Z1-D1)*Q1(JL)
      FT(K3)=G(JL)+ATRI1
  254 GO TO (361,363),LAPPA
   47 ANU3=ANU1-CINTST
      Q2(K2)=((((BE-1.0)**2)*(SIN(((CA+0.5*PAI)*DJ/TAU)-CA))**4+
     1 ((VK+RUN)/UL)**2)**0.25)*ANU3
  256 IF(Q2(K2).LT.0.0) GO TO 610
  609 IF(DJ.LT.DLTSTR) GO TO 250
```

```
          IF((DJ.GT.DLTSTR).AND.(DJMDST.LT.DDELT)) GO TO 206
          GO TO 250
      206 IF(MISA.EQ.2) GO TO 203
      250 DJ=DJ+DDELT
      620 CONTINUE
      623 WRITE(6,624)
      624 FORMAT(10X,29H NU1 DOES NOT BECOME NEGATIVE)
          STOP
      610 KK=K2-1
          MILLA=1
          IF(DJMDST.LT.DDELT) GO TO 221
          IF((DJMDST.LT.(2*DDELT)).AND.(DJMDST.GT.DDELT)) GO TO 237
          GO TO 238
      237 KK=K2-1
          G(MILLA)=0.0
          CALL QSF(DDELT,Q1,G,LASTK)
          Q1INT=G(LASTK)
          GO TO 239
      238 IF((DJMDST.LT.(3*DDELT)).AND.(DJMDST.GT.(2*DDELT))) GO TO 241
          GO TO 55
      241    Q2INT=(Q2(LIRSTK)+Q2(KK))*DDELT*0.5
          CALL QSF(DDELT,Q1,G,LASTK)
          Q1INT=G(LASTK)
          GO TO 239
      221 Q2(KK)=STAR2
      236 CALL QSF(DDELT,Q1,G,LASTK)
          Q1INT=G(LASTK)
      234 AREA1=(Q1(LASTK)+ Q1STR)*(DDELT-SECT)/2.0
          DD=DLTSTR
          Z=((DD)*Q2(K2)-DJ*Q2(KK))/(Q2(K2)-Q2(KK))
          ATRI=0.5*(Z-DD)*Q1STR
          AREA2=0.0
          G(MILLA)=0.0
          GO TO 631
       55 MILLA=KK-LASTK
          DO 61 NNL=1,MILLA
       61 Q3(NNL)=Q2(LASTK+NNL)
          CALL QSF(DDELT,Q1,G,LASTK)
          Q1INT=G(LASTK)
          CALL QSF(DDELT,Q3,G,MILLA)
          Q2INT=G(MILLA)
      239 AREA1=(Q1(LASTK)+ Q1STR)*(DDELT-SECT)/2.0
          AREA2=((Q2(LIRSTK)+ STAR2)*SECT)/2.0
          DD=DJ-DDELT
          Z=((DD)*Q2(K2)-DJ*Q2(KK))/(Q2(K2)-Q2(KK))
          ATRI=0.5*(Z-DD)*Q2(KK)
      631 FT(K3)=Q1INT+Q2INT+AREA1+AREA2+ATRI
      257 GO TO (361,363),LAPPA
      361 PSI(K3)=COEF*(2.0*(TI**EN)-EN*(TI**2))/(EN-2.0)
      363 GO TO (699,899),LIRA
      899 V(K3)=VK+PSI(K3)
          SMALLG(K3)=AC+BC*V(K3)-DC*(1.0+0.5*V(K3))*FT(K3)
          IF(K3.EQ.1) GO TO 903
          MAL=K3-1
          CAPG(K3)=(SMALLG(K3)+SMALLG(MAL))*DTETA/2.0+CAPG(MAL)
          CAPG(ITETP)=0.0
```

```
0270          GO TO 904
0271      903 CAPG(K3)=0.0
0272          GO TO 632
0273      904 PROD=SMALLG(K3)*SMALLG(MAL)
0274      998 IF((K3.EQ.ITETP).AND.(MINA.EQ.1)) GO TO 900
0275          IF(PROD.LT.0.0) GO TO 831
0276          GO TO 632
0277      831 ZFGO=TI-ABS((DTETA*SMALLG(K3))/(ABS(SMALLG(K3))+ABS(SMALLG(MAL
             1))))
0278          STORM1=TI-DTETA
0279          ZATRI=(ZFGO-STORM1)*SMALLG(MAL)/2.0
0280          PATRI=(TI-ZFGO)*SMALLG(K3)/2.0
0281          QUAD=PATRI+ZATRI
0282          CAPG(K3)=CAPG(MAL)+QUAD
0283          WRITE(6,444) CAPG(K3)
0284      444 FORMAT(1X,8H CAPG = ,1PE16.6)
0285          GO TO (842,843,560,561,562,563),LAMA
0286      842 CGST1=CAPG(MAL)+ZATRI
0287          ZFGO1=ZFGO
0288      564 CAPGST=CGST1
0289          TISTAR=ZFGO1
0290          WRITE(6,540) ZFGO1
0291      540 FORMAT(1X,9H ZFGO1 = ,1PE16.6)
0292          LAMA=2
0293          GO TO 632
0294      843 CGST2=CAPG(MAL)+ZATRI
0295          ZFGO2=ZFGO
0296          WRITE(6,550) ZFGO2
0297      550 FORMAT(1X,9H ZFGO2 = ,1PE16.6)
0298          LAMA=3
0299          IF(CGST1.LT.CGST2) GO TO 632
0300          CAPGST=CGST2
0301          TISTAR=ZFGO2
0302          GO TO 632
0303      560 CGST3=CAPG(MAL)+ZATRI
0304          ZFGO3=ZFGO
0305          LAMA=4
0306          IF(CAPGST.GT.CGST3) GO TO 565
0307          GO TO 632
0308      565 CAPGST=CGST3
0309          TISTAR=ZFGO3
0310          GO TO 632
0311      561 CGST4=CAPG(MAL)+ZATRI
0312          ZFGO4=ZFGO
0313          LAMA=5
0314          IF(CAPGST.GT.CGST4) GO TO 566
0315          GO TO 632
0316      566 CAPGST=CGST4
0317          TISTAR=ZFGO4
0318          GO TO 632
0319      562 CGST5=CAPG(MAL)+ZATRI
0320          ZFGO5=ZFGO
0321          LAMA=6
0322          IF(CAPGST.GT.CGST5) GO TO 567
0323          GO TO 632
0324      567 CAPGST=CGST5
```

```
          TISTAR=ZFGC5
          GO TO 632
      563 CGST6=CAPG(MAL)+ZATRI
          ZFGO6=ZFGO
          IF(CAPGST.GT.CGST6) GO TO 568
          GO TO 632
      568 CAPGST=CGST6
          TISTAR=ZFGO6
      699 V(K3)=VK+PSI(K3)
          SMALLG(K3)=AC+BC*V(K3)-DC*(1.0+0.5*V(K3))*FT(K3)
      632 TI=TI+DTETA
      700 CONTINUE
          CALL QSF(DTETA,SMALLG,G,ITETP)
          TIC(I)=G(ITETP)
          WRITE(6,283) TIC(I)
      283 FORMAT(20X,7H TIC = ,1PE16.6)
     9976 GO TO (802,803),MARY
      802 IF(I.EQ.1) GO TO 801
          IM=I-1
          TEST=TIC(I)*TIC(IM)
          IF(TEST.LT.0.0) GO TO 805
      801 VK=VK+VINT
          IF((I.EQ.1).AND.(TIC(I).GT.0.0)) GO TO 248
          IF(I.EQ.JVNB) GO TO 248
          GO TO 800
      248 STOP
      800 CONTINUE
      805 GIC1=TIC(IM)
          GIC2=TIC(I)
      810 X1=VK-VINT
          X2=VK
      812 X=(X1*GIC2-X2*GIC1)/(GIC2-GIC1)
          VK=X
          MARY=2
          GO TO 26
      803 WRITE(6,729)
      729 FORMAT(50X,8H M(TETA))
          WRITE (6,730) (FT(K3),K3=1,ITETP)
      730 FORMAT(47X,1PE16.6)
          LIRA=2
          MAMA=1
          GO TO 26
      900 IF(LAMA.EQ.1) GO TO 262
          IF(LAMA.EQ.2) GO TO 263
          GO TO 264
      262 WRITE(6,268)
      268 FORMAT(/20X,26H SMALLG(K3) DOES NOT CROSS)
          STOP
      263 IF(CGST1.GT.0.0) GO TO 266
          GO TO 267
      266 WRITE(6,269)
      269 FORMAT(/20X,42H SMALLG(K3) CROSSES ONCE BUT CGST1 GT ZERO)
      267 CAPGST=CGST1
          TISTAR=ZFGO1
      264 WRITE(6,571) CAPGST,TISTAR
      571 FORMAT(2X,10H CAPGST = ,1PE16.6,10H TISTAR = ,1PE16.6)
```

```
      921 IF(CAPGST.LT.0.0) GO TO 923
          WRITE(6,922)
      922 FORMAT(//50X,25H G(TETA STAR) IS POSITIVE)
          STOP
      923 VAVRG=VK-(-(2.0*CAPGST))**0.5
          WRITE(6,924) VAVRG
      924 FORMAT(1X,8H V(M) = ,1PE16.6)
          WRITE(6,970) TI
      970 FORMAT(1X,6H TI = ,F7.4)
          THI=0.0
          DO 931 LL=1,ITETP
          UNO=(VK-VAVRG)**2+2.0*CAPG(LL)
          IF(UNO.GE.0.0) GO TO 928
          WRITE(6,927)
      927 FORMAT(/20X,22H V1(TETA) IS IMAGINARY)
          STOP
      928 IF(THI.LT.TISTAR) V1(LL)=VAVRG+UNO**0.5
          IF(THI.GT.TISTAR) V1(LL)=VAVRG-UNO**0.5
          IF(LAST.EQ.1) GO TO 292
          DIF(LL)=ABS(V2(LL)-V1(LL))
      292 CRI(LL)=V1(LL)-VK
          PSI(LL)=(CRI(LL)+PSI(LL))/2.0
          V2(LL)=V1(LL)
          V1SQ(LL)=V1(LL)*V1(LL)
          WRITE(6,929) V1(LL) ,LL,CRI(LL)
      929 FORMAT(1X,12H V1(TETA) = ,1PE16.6,2X,6H K3 = ,I4,
        13X,12H PSI1(K3) = ,1PE14.6)
          THI=THI+DTETA
      931 CONTINUE
          IF (LAST.EQ.1) GO TO 385
          DO 380 NN=1,ITETP,5
          WRITE(6,293) DIF(NN)
      293 FORMAT(//10X,7H DIF = ,1PE16.6)
          IF(DIF(NN).LT.0.0010) GO TO 380
          GO TO 385
      380 CONTINUE
          CALL QSF(DTETA,V1SQ,G,ITETP)
          ENERGY=G(ITETP)
          WRITE(6,3901) ENERGY
     3901 FORMAT(50X,10H ENERGY = ,1PE16.4)
          WRITE(6,390)
      390 FORMAT(/////50X,17H BRAVO GIOVANNINO)
          GO TO 399
      385 LAPPA=2
          LAST=2
          VK=VKAPPA
          GO TO 15
      399 STOP
          END
```

APPENDIX B

Program Outline For Transient Solutions

The nonlinear integro-differential Eq.(29), after the formal simplifications seen in Section 3.1, will read as follows:

$$(v - v_m)\frac{\partial v}{\partial \theta} = A + Bv(\theta, t) - D\left[1 + \frac{v(\theta, t)}{2}\right] M(\theta, t) + \frac{2}{\gamma + 1}\frac{\partial v}{\partial t} \tag{I}$$

Let us call again:

$$A + Bv(\theta, t) - D\left[1 + \frac{v(\theta, t)}{2}\right] M(\theta, t) = g(\theta, t)$$

thus, (I) becomes:

$$(v - v_m)\frac{\partial v}{\partial \theta} = g + \frac{2}{\gamma + 1}\frac{\partial v}{\partial t} \tag{II}$$

The easiest way to think of a solution for this nonlinear partial integro-differential equation (any other method such as the method of characteristics, is made very hard by the unknown behavior of the rather complicated form of $g(\theta, t)$) is to write Eq. II as follows:

$$(v - v_m)\frac{\Delta v}{\Delta \theta} = g + \frac{2}{\gamma + 1}\frac{\Delta v}{\Delta t} \tag{III}$$

For a given solution of the wave equation at $t = t_o$ and for some given Δt, we are able to find at $t = t_o + \Delta t$ a new wave solution as long as we regard the equation dependent on θ only.

To give now an expression for Δt let us consider:

$$\theta = ft - y$$

The shock velocity is given by: $dy/dt = f$ or, considering finite increments, by $\Delta y/\Delta t = f$. For a period, $\Delta y = 1$ then: $\Delta t = 1/f$ where $f = 1 + \frac{\gamma+1}{2} v_m$. With these elements it is easy to work with the iteration procedure as it has been done in the case of periodic solutions.

It must be understood that great care has to be taken in defining $\Delta v/\Delta t$ in that portion of the transverse velocity distribution which experiences the steepest slope (i.e., for early values of θ). It should be wise to take values of $\Delta\theta$ as small as possible to approach a smooth v_θ distribution along the period from 0 to 1.

JP 21 R 4334 68 b

Transverse mode combustion instability

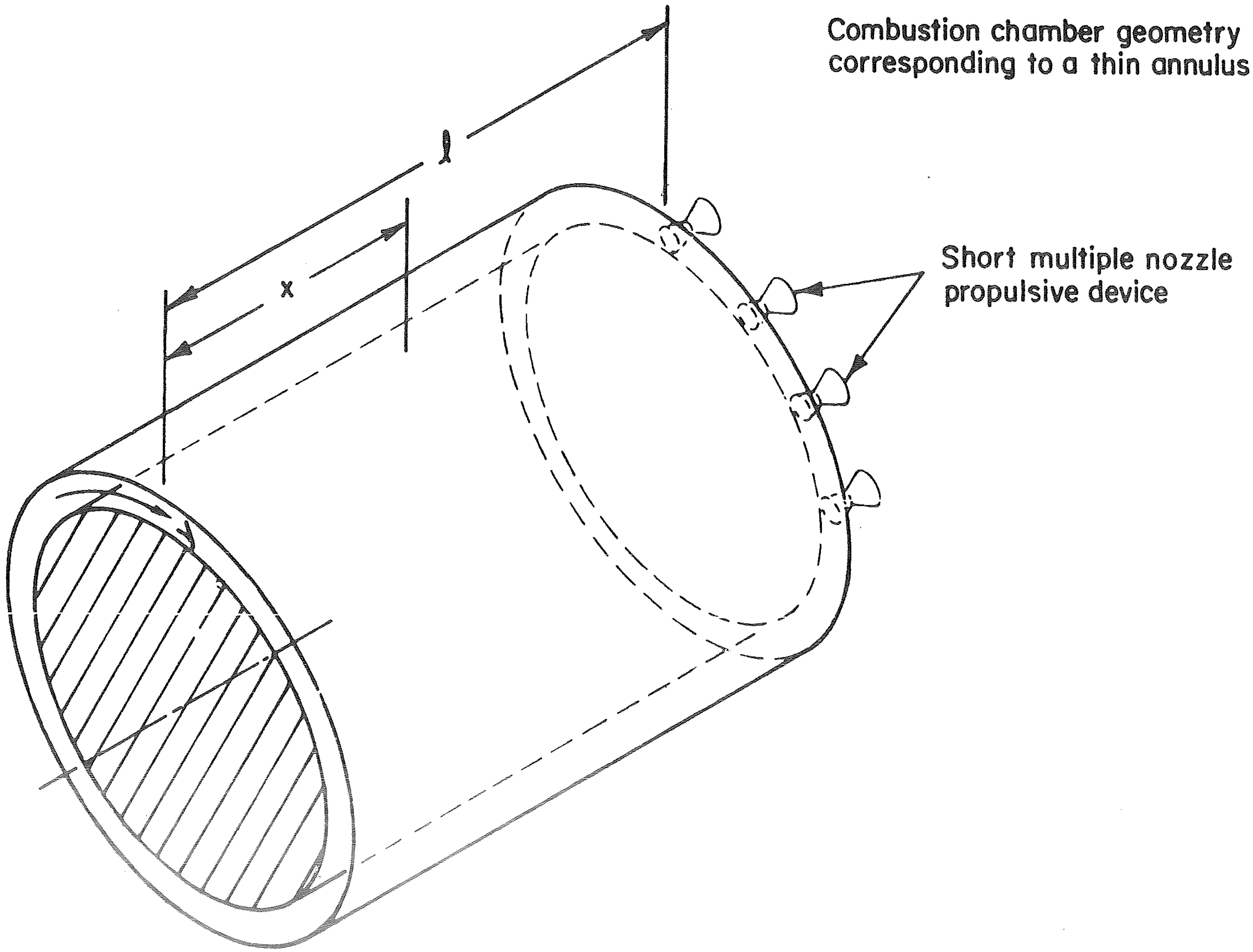

Figure 1

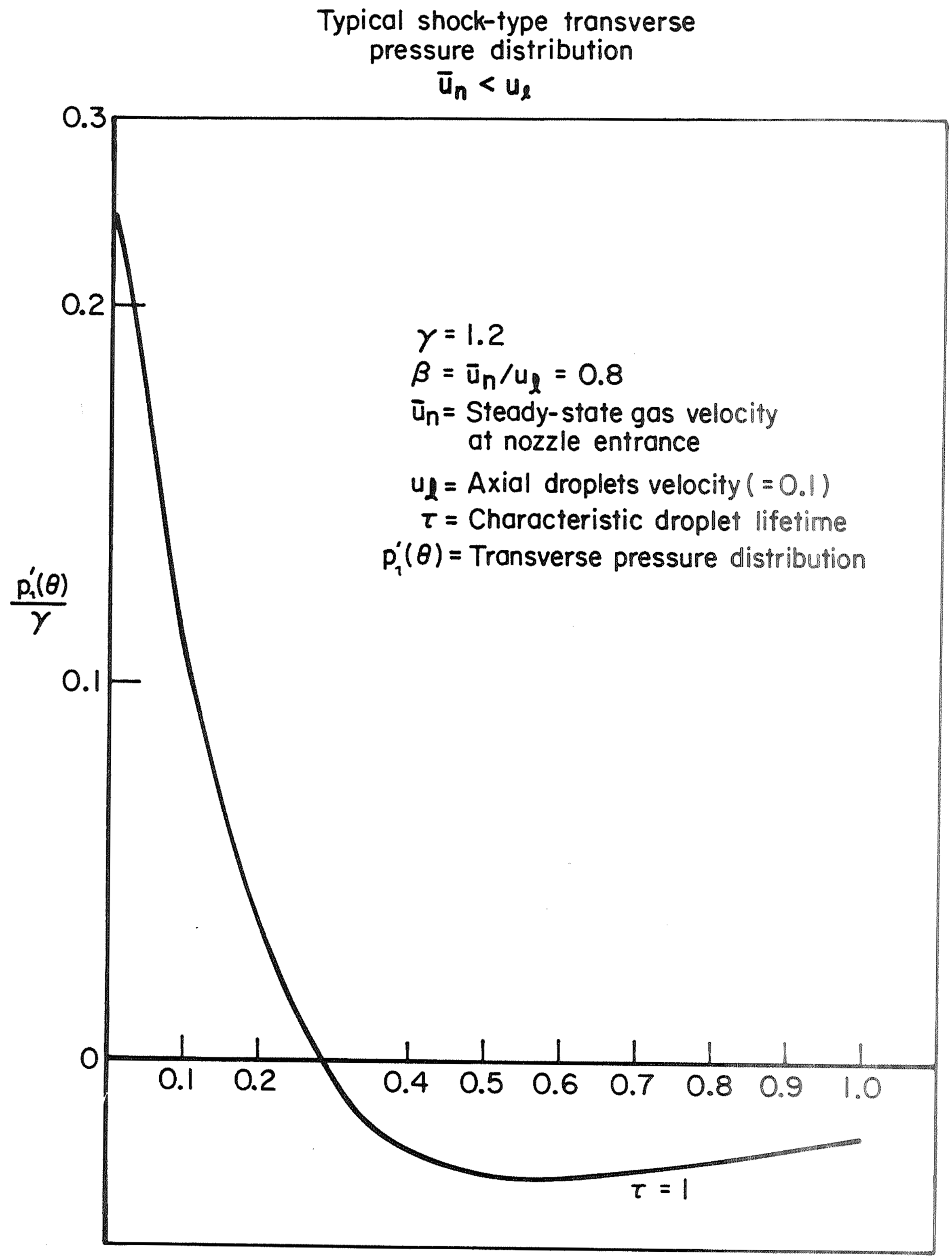

Figure 2

6114 2 125 71

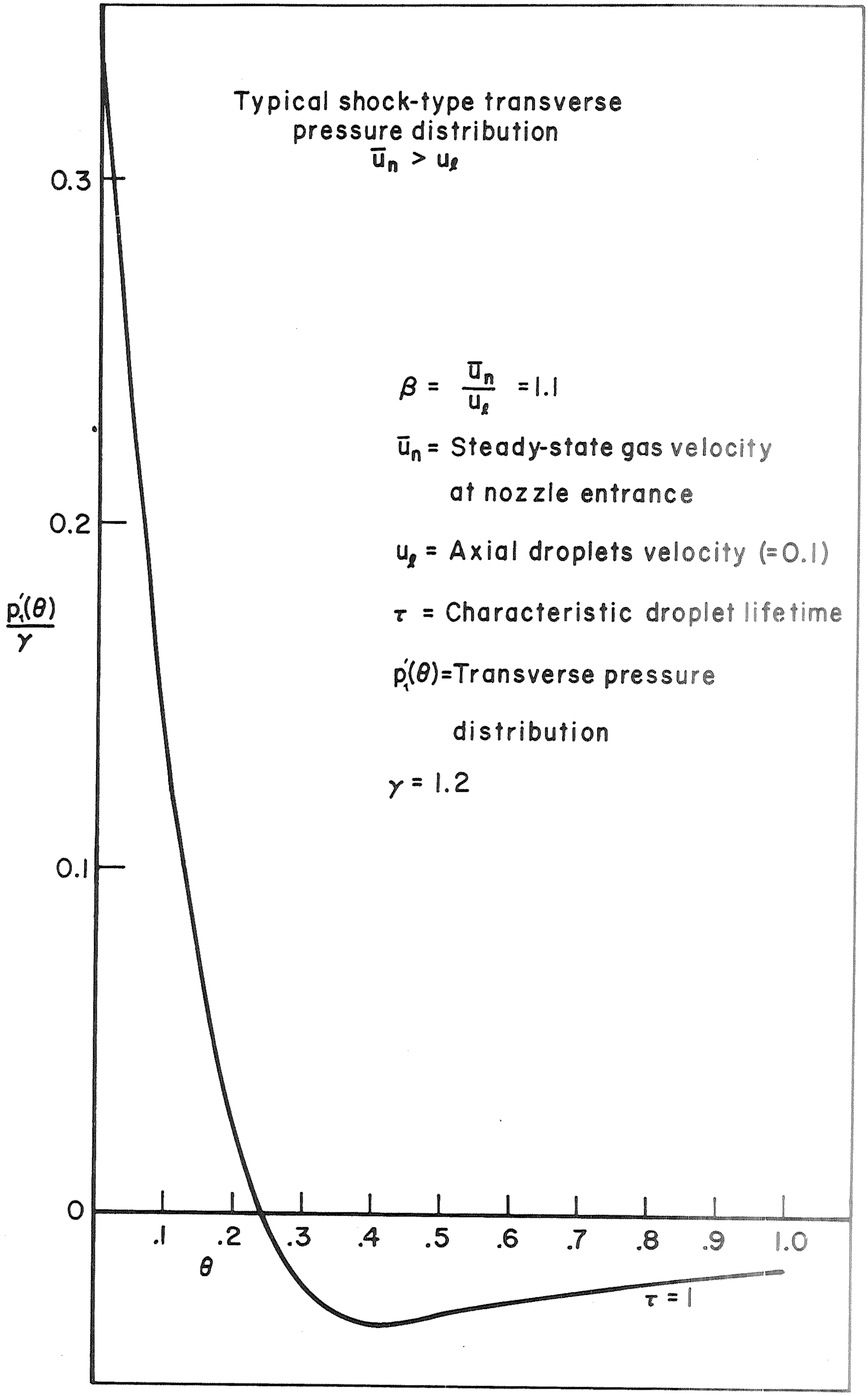

G114 R 126 71

Figure 3

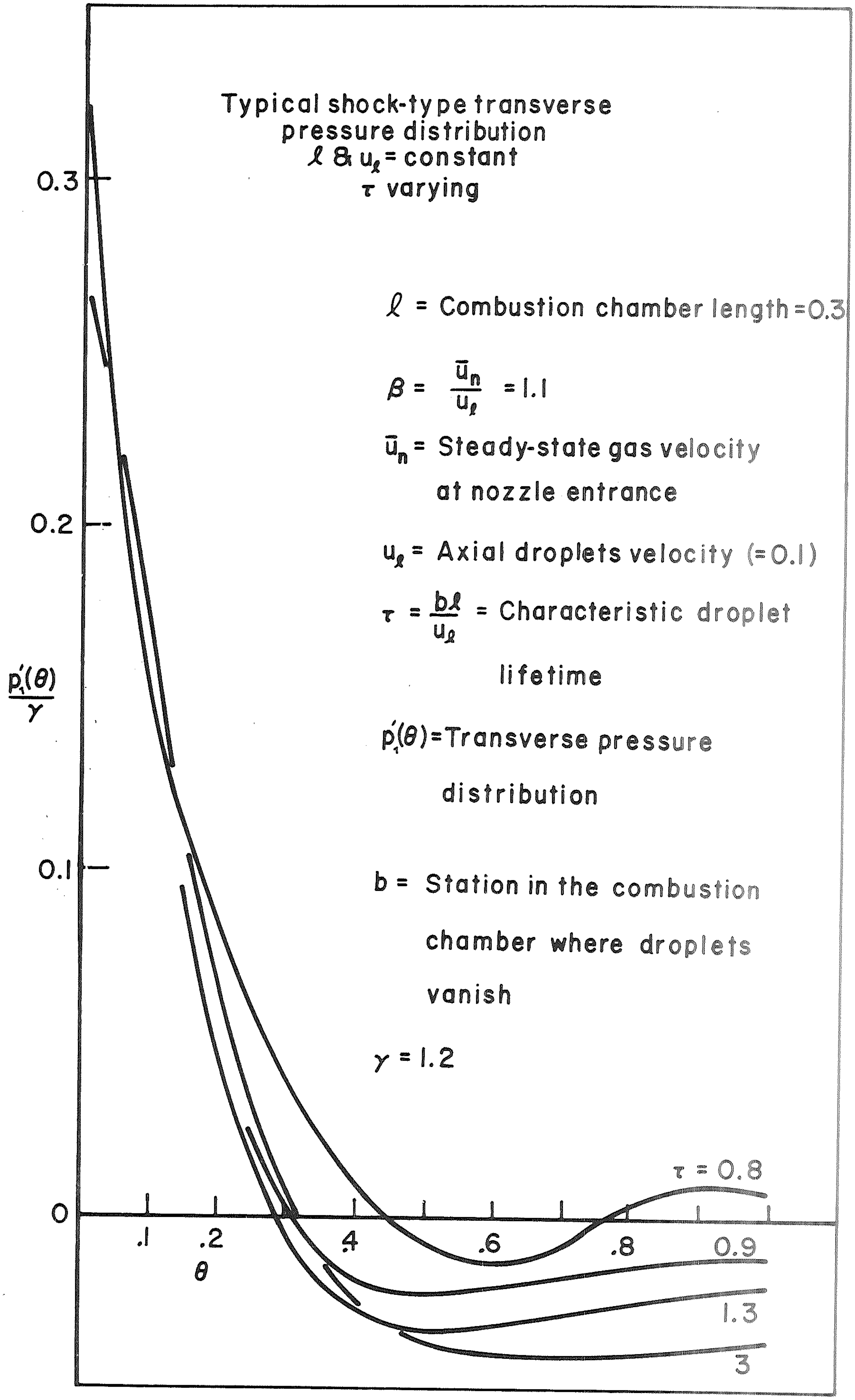
Typical shock-type transverse
pressure distribution
ℓ & u_ℓ = constant
τ varying
ℓ = Combustion chamber length = 0.3
$\beta = \frac{\bar{u}_n}{u_\ell} = 1.1$
$\bar{u}_n$ = Steady-state gas velocity at nozzle entrance
u_ℓ = Axial droplets velocity (=0.1)
$\tau = \frac{b\ell}{u_\ell}$ = Characteristic droplet lifetime
$p_1'(\theta)$ = Transverse pressure distribution
b = Station in the combustion chamber where droplets vanish
$\gamma = 1.2$
$\frac{p_1'(\theta)}{\gamma}$
0.3
0.2
0.1
0
.1
.2
.4
.6
.8
θ
τ = 0.8
0.9
1.3
3

Figure 4

6114 R 129 71

Shock energy versus droplet lifetime

$\bar{u}_n < u_\ell$

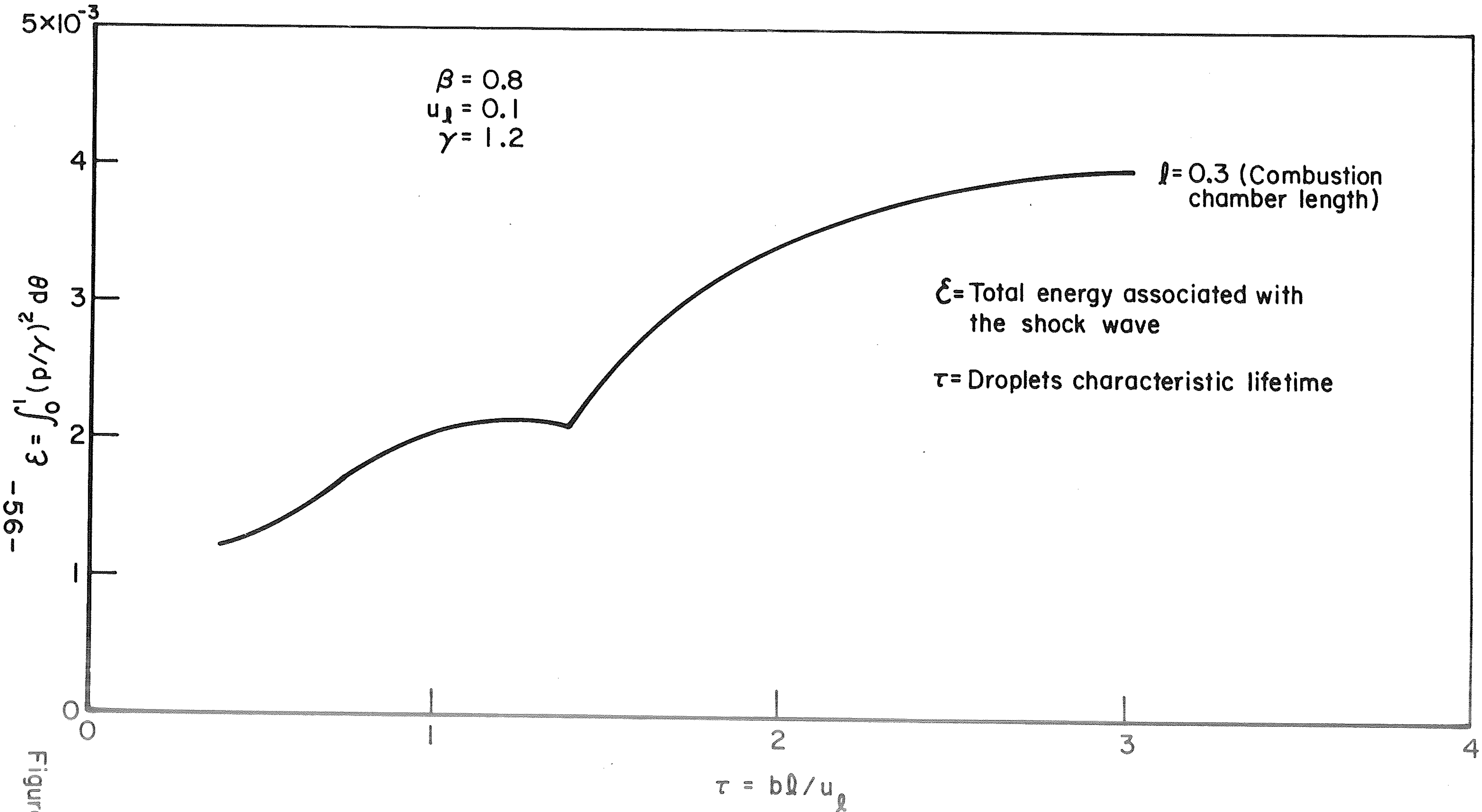

Figure 5

6114 R 130 T1

Energy in transverse mode combustion instability, $\mathcal{E}$, versus droplet lifetime with $\bar{u}_n > u_\ell$, ℓ varying

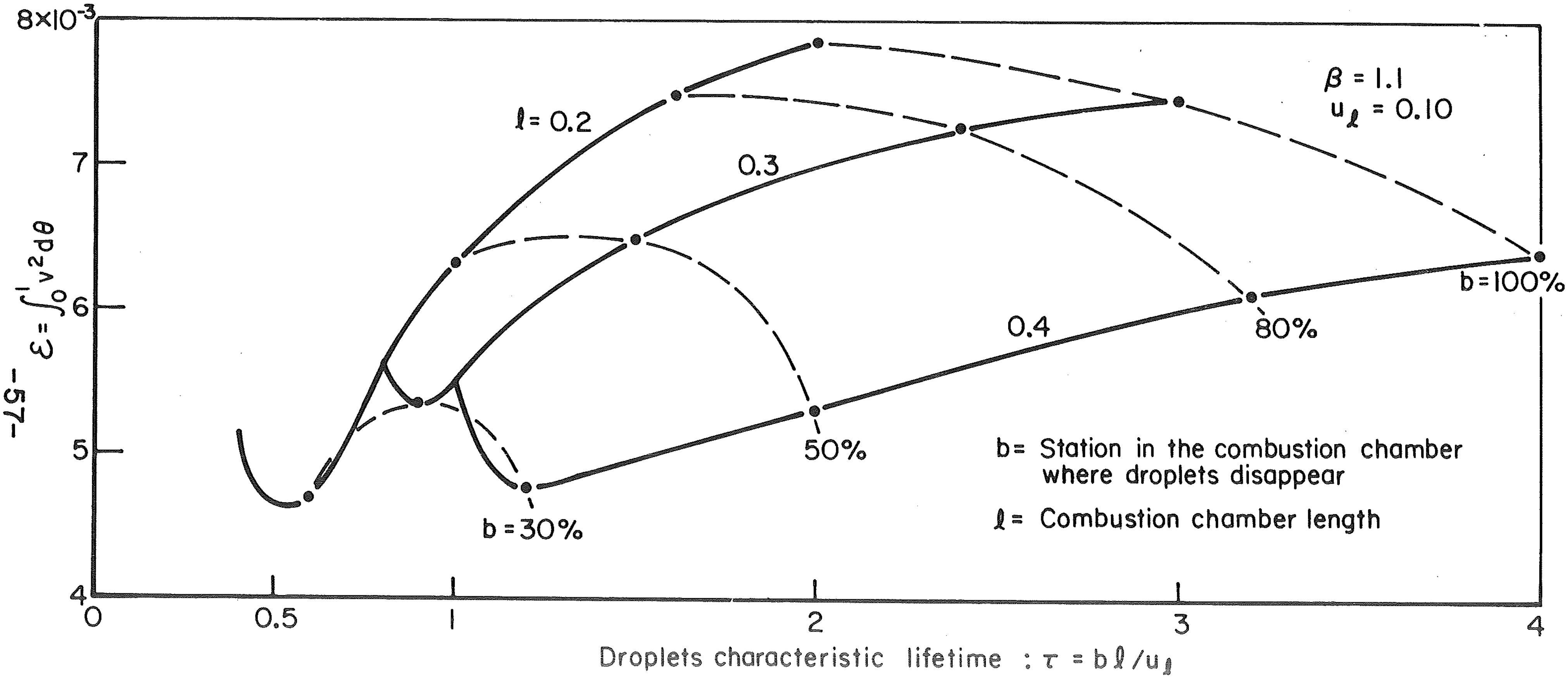

Figure 6

Energy in transverse mode combustion instability, $\mathcal{E}$, versus droplet lifetime with ℓ and β constant, u_ℓ varying

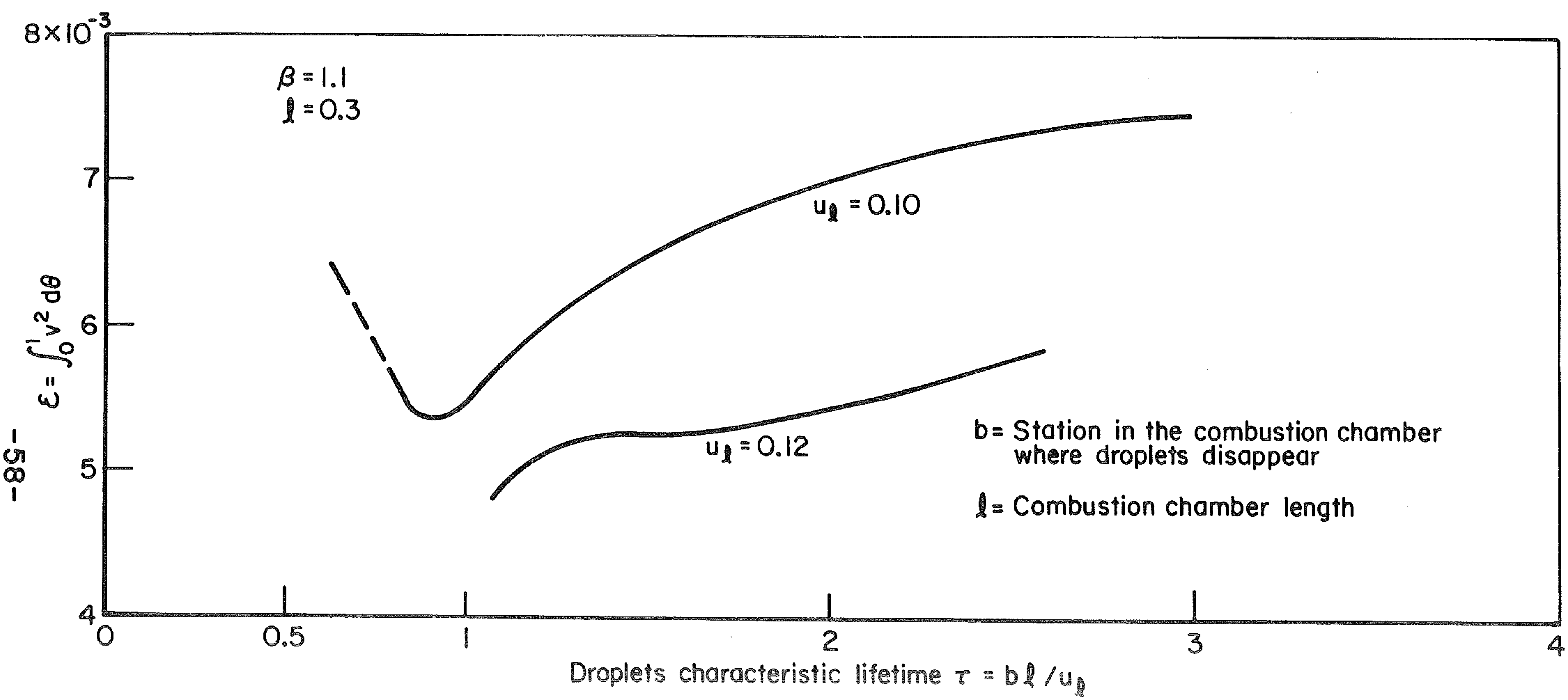

Figure 7

1972 DISTRIBUTION LIST

Dr. R.J. Priem MS 500-209
NASA Lewis Research Center
21000 Brookpark Road
Cleveland, Ohio 44135 (2)

Marcus F. Heidmann
NASA Lewis Research Center
21000 Brookpark Road
Cleveland, Ohio 44135

Norman T. Musial
NASA Lewis Research Center
21000 Brookpark Road
Cleveland, Ohio 44135

Library
NASA Lewis Research Center
21000 Brookpark Road
Cleveland, Ohio 44135 (2)

Report Control Office
NASA Lewis Research Center
21000 Brookpark Road
Cleveland, Ohio 44135

E.W. Conrad MS 500-204
NASA Lewis Research Center
21000 Brookpark Road
Cleveland, Ohio 44135

L. Gordon MS 500-209
NASA Lewis Research Center
21000 Brookpark Road
Cleveland, Ohio 44135

NASA Representative
NASA Scientific and Technical
Information Facility
P.O. Box 33
College Park, Maryland 20740
(2 copies with Document
Release Authorization Form)

R.S. Levine MS 213
NASA
Langley Research Center
Hampton, Virginia 23365

R.J. Richmond SNE-ASTN-PP
NASA George C. Marshall Space
Flight Center
Huntsville, Alabama 35812

J. G. Thibadaux
NASA Manned Spacecraft Center
Houston, Texas 77058

R.R. Weiss
AFRPL
Edwards, California 93523

National Technical Information
Service
Springfield, Virginia 22151 (40)

J. H. Rupe
Jet Propulsion Laboratory
California Institute of
Technology
4800 Oak Grove Drive
Pasadena, California 91103

F.E. Culick
California Institute of
Technology
Pasadena, California 91109

R. Edse
Ohio State University
Dept. of Aeronautical and
Astronautical Engineering
Columbus, Ohio 43210

G.M. Faeth
The Pennsylvania State University
Mechanical Engineering Dept.
207 Mechanical Engineering Blvd.
University Park, Pa. 16802

M. Gerstein
Dept. of Mechanical Engineering
University of Southern California
University Park
Los Angeles, California 90007

C.E. Mitchell
Colorado State University
Mechanical Engineering Dept.
Fort Collins, Colorado 80521

P.S. Myers
University of Wisconsin
Mechanical Engineering Department
1513 University Avenue
Madison, Wisconsin 53706

J. A. Nicholls
University of Michigan
Aerospace Engineering
Ann Arbor, Michigan 48104

J. C. O'Hara
Tulane University
Department of Mechanical Engineering
New Orleans, La. 70118

A.K. Oppenheim
University of California
Department of Aeronautical Sciences
6161 Etcheverry Hall
Berkeley, California 94720

K. Ragland
University of Wisconsin
Mechanical Engineering Department
Madison, Wisconsin 53705

A.A. Ranger
Purdue University
School of Aeronautics, Astronautics and Engr. Sciences
Lafayette, Indiana 47907

F.H. Reardon
Sacramento State College
School of Engineering
6000 J. Street
Sacramento, California 95819

B.A. Reese
Purdue University
School of Mechanical Engineering
Lafayette, Indiana 47907

R.F. Sawyer
University of California
Mechanical Engineering, Thermal Systems
Berkeley, California 94720

R.A. Strehlow
University of Illinois
Aeronautics/Astronautic Engineering Department
Transportation Bldg., Rm. 101
Urbana, Illinois 61801

T.P. Torda
Illinois Institute of Technology
Room 200 M.H.
3300 S. Federal Street
Chicago, Illinois 60616

W.E. Strahle
Aerospace School
Georgia Institute of Technology
Atlanta, Georgia 30332

T.Y. Toong
Massachusetts Institute of Technology
Department of Mechanical Engr.
Cambridge, Massachusetts 02139

F.A. Williams
University of California
Aerospace Engineering Dept.
P.O. Box 109
La Jolla, California 92037

B.T. Zinn
Georgia Institute of Technology
Aerospace School
Atlanta, Georgia 30332

P.F. Winternitz
New York University
University Heights
New York, New York

Library
Stanford Research Institute
333 Ravenswood Avenue
Menlo Park, California 94025

R. Goulard
Purdue University
School of Mechanical Engineering
Lafayette, Indiana 47907

Marshall Industries
Dynamic Science Division
2400 Michelson Drive
Irvine, California 92664
Attn: L. Zung

T.W. Christian
Johns Hopkins University/APL
Chemical Propulsion Information Agency
8621 Georgia Avenue
Silver Spring, Maryland 20910

O.W. Dykema
Aerospace Corporation
P.O. Box 95085
Los Angeles, California 90045

Library
Director (Code 6180)
U. S. Naval Research Laboratory
Washington, D.C. 20390

TISIA
Defense Documentation Center
Cameron Station
Building 5
5010 Duke Street
Alexandria, Virginia 22314

Office of Asst. Director
Chemical Technology
Office of the Director of Defense
Research and Engineering
Washington, D.C. 20310

D.E. Mock
Advanced Research Projects Agency
Washington, D.C. 20525

H.K. Doetsch
Arnold Engineering Development
Center
Air Force Systems Command
Tullahoma, Tennessee 37389

I. Forsten
Picatinny Arsenal
Dover, New Jersey 07801

Naval Underwater Systems Center
Energy Conversion Department
Attn: R.S. Lazar
Code TB 131
Newport, Rhode Island 02840

V. Agosta
Brooklyn Polytechnic Institute
Long Island Graduate Center
Route 110
Farmingdale, New York 11735

R.M. Clayton
Jet Propulsion Laboratory
California Institute of Technology
4800 Oak Grove Drive
Pasadena, California 91103

E.K. Dabora
University of Connecticut
Aerospace Department
Storrs, Connecticut 06268

T.F. Ferger
Bell Aerospace Co.
P.O. Box 1
Mail Zone J-81
Buffalo, New York 14205

Technical Information Dept.
Aeronutronic Division of
Philco Ford Corporation
Newport Beach, California 92663

D. Suichu
General Electric Company
Flight Propulsion Lab. Dept.
Cincinnati, Ohio 45215

Library
Ling-Temco-Vought Corporation
P. O. Box 5907
Dallas, Texas 75222

Marquardt Corporation
16555 Saticoy Street
Box 2013 - South Annex
Van Nuys, California 91409

Library-Susquehanna Corp.
Atlantic Research Division
Shirley Highway & Edsall Road
Alexandria, Virginia 23314

David Altman
United Aircraft Corporation
United Technology Center
P. O. Box 358
Sunnyvale, California 94088

Report Library
Room 6A
Battelle Memorial Institute
505 King Avenue
Columbus, Ohio 43201

Dipl-Ing. Hans G. Ruppik
DEVLR Institut fur Chemische
Raketenantriebe
7101 Lampoldshausen/Wurtt
Germany

J. B. Large
Institute of Sound and Vibration
Research
University of South Hampton
England

Library - Documents
Aerospace Corporation
2400 E. El Segundo Blvd.
Los Angeles, California 90045

G.W. Elverum
TRW Systems
One Space Park
Redondo Beach, California 90278

STL Tech. Library
Document Acquisitions
TRW Systems Group
One Space Park
Redondo Beach, California 90278

G.D. Garrison
Pratt and Whitney Aircraft
Florida Research and Development Center
P.O. Box 710
West Palm Beach, Florida 33402

Library
United Aircraft Corporation
Pratt and Whitney Division
Florida Research & Development Center
P. O. Box 710
West Palm Beach, Florida 33402

J.M. McBride
Aerojet-General Corporation
P. O. Box 15847
Sacramento, California 95809

R. Stiff
Propulsion Division
Aerojet-General Corporation
P. O. Box 15847
Sacramento, California 95803

J.A. Nestlerode
AC46 D/596-121
North American Rockwell Corp.
Rosketdyne Division
6633 Canoga Avenue
Canoga Park, California 91304

T.A. Coultas D991-350
North American Rockwell Corp.
Rocketdyne Division
Zone 11
6633 Canoga Avenue
Canoga Park, California 91304

L. M. Wood
Bell Aerospace Company
P. O. Box 1
Mail Zone J-81
Buffalo, New York 14205

Library
Air Force Rocket Propulsion Laboratory (RPM)
Edwards, California 93523

R.W. Haffner
Air Force Office of Scientific Research
1400 Wilson Blvd.
Arlington, Virginia 22209

K. Scheller
ARL (ARC)
Wright-Patterson AFB
Dayton, Ohio 45433

Air Force Aero Propulsion Laboratory
Attn: APTC Lt. M. Johnson
Wright Patterson AFB
Dayton, Ohio 45433

J.R. Osborn
Army Ballistics Laboratories
Aberdeen Proving Ground
Maryland 21005

D. H. Dahlene
Attn: AMSMI-RK
U.S. Army Missile Command
Redstone Arsenal
Alabama 35808

T. Inouye
Code 4581
U.S. Naval Weapons Center
China Lake, California 93555

R.D. Jackel 473
Office of Naval Research
Navy Department
Washington, D.C. 20360

Library
Bureau of Naval Weapons
Department of the Navy
Washington, D.C.

A.P. Chervinsky
Dept. of Aeronautical Engineering
Technion Israel Institute of Technology
Haifa, Israel

J.S. T'ien
School of Engineering
Division of Fluid, Thermal and
Aerospace Sciences
Case Western Reserve University
Cleveland, Ohio 44106